

See discussions, stats, and author profiles for this publication at: <https://www.researchgate.net/publication/231231136>

Regulation and Properties of Diversiform Cd(II) Supramolecular Complexes with a Bulky Naphthalene-Based Dicarboxyl Tecton and Different N-Donor Co-Ligands

ARTICLE *in* CRYSTAL GROWTH & DESIGN · SEPTEMBER 2010

Impact Factor: 4.89 · DOI: 10.1021/cg100645p

CITATIONS

47

READS

25

7 AUTHORS, INCLUDING:



Min Hu

Zhengzhou University of Light Industry

54 PUBLICATIONS 375 CITATIONS

[SEE PROFILE](#)



Miao Du

Tianjin Normal University

307 PUBLICATIONS 8,847 CITATIONS

[SEE PROFILE](#)



Chun-Sen Liu

Zhengzhou University of Light Industry

94 PUBLICATIONS 1,589 CITATIONS

[SEE PROFILE](#)

Regulation and Properties of Diversiform Cd(II) Supramolecular Complexes with a Bulky Naphthalene-Based Dicarboxyl Tecton and Different *N*-Donor Co-Ligands

Shao-Ming Fang,[†] Qiang Zhang,[†] Min Hu,[†] Xiao-Gang Yang,[†] Li-Ming Zhou,[†] Miao Du,^{*,‡} and Chun-Sen Liu^{*,†}

[†]Zhengzhou University of Light Industry, Henan Provincial Key Laboratory of Surface & Interface Science, Zhengzhou, Henan 450002, P. R. China, and [‡]College of Chemistry, Tianjin Key Laboratory of Structure and Performance for Functional Molecule, Tianjin Normal University, Tianjin 300387, P. R. China

Received May 14, 2010; Revised Manuscript Received August 15, 2010

ABSTRACT: A series of six Cd^{II} coordination complexes have been prepared by using naphthalene-2,3-dicarboxylic acid (H₂**ndc**), an analogue of 1,2-benzenedicarboxylic acid (H₂**bdc**), and different *N*-donor auxiliary co-ligands (chelating or bridging), namely, [Cd(**ndc**)₂]_∞ (**1**), {[Cd₂(**ndc**)₂(2bpy)₂(H₂O)₂](CH₃OH)_{0.5}}₂ (**2**), [Cd₂(**ndc**)₂(phen)₂]_∞ (**3**), {[Cd(**ndc**)(4bpy)_{0.5}(H₂O)₂](H₂O)}_∞ (**4**), {[Cd(**ndc**)(abp)(H₂O)](H₂O)}_∞ (**5**), and {[Cd(**ndc**)(bpp)₂](H₂O)₃]_∞ (**6**) (**ndc** = naphthalene-2,3-dicarboxylate, 2bpy = 2,2'-bipyridine, phen = 1,10-phenanthroline, 4bpy = 4,4'-bipyridine, abp = *trans*-4,4'-azobis(pyridine), and bpp = 1,3-bis(4-pyridyl) propane). The initial complex **1** shows a two-dimensional (2-D) (4⁴.6²) coordination network. **2** and **3** possess tetranuclear and one-dimensional (1-D) structures due to the incorporation of auxiliary chelating co-ligands 2bpy and phen, respectively, which are further interlinked via secondary interactions such as hydrogen bonding and aromatic stacking to result in higher-dimensional supramolecular networks. When the 4,4'-dipyridyl-type bridging co-ligands 4bpy, abp, and bpp (with different *N,N'*-donor separations of the molecular backbones from ca. 7–10 Å) were used as the additional rod-like linkers, a 2-D (3,4)-connected (4².6)(4².6³.8) layered coordination net **4** as well as a three-dimensional (3-D) coordination framework **5** with an unusual 4-connected **irl** topology (4².6³.8) and a homochiral 3-D diamond (**dia**) network **6** were obtained. A structural comparison of these complexes with those based on the structurally related ligand 1,2-benzenedicarboxylate (**bdc**) suggests that the extended π-conjugated system of **ndc** with a different electronic nature and steric bulk plays an important role in the construction of supramolecular architectures for **1**–**6**, which can also be well regulated by the different chelating or bridging *N*-donor co-ligands. Moreover, complexes **1**–**6** exhibit strong solid-state luminescence emissions at room temperature, which mainly originate from the intraligand π → π* transitions of **ndc**.

Introduction

In recent years, extensive experimental and theoretical efforts have been focused on the rational design and controlled synthesis of metal–organic frameworks (MOFs),¹ also known as coordination polymers, from predesigned bridging ligands and metal ions, because such hybrid materials can exhibit a variety of regulated and interesting structural topologies^{2,3} as well as many potential applications in photoluminescence,⁴ magnetism,⁵ catalysis,⁶ gas storage,⁷ conductivity,⁸ nonlinear optics (NLO),⁹ ion exchange,¹⁰ ferroelectricity,¹¹ optoelectronic effect,¹² and spin-transition behavior.¹³ In this field, several synthetic strategies have been developed to achieve the targeting assemblies of such extended crystalline systems with desired structural features and/or physicochemical properties,^{1–13} among which the appropriate choice of well-designed organic building blocks and metal ions or clusters is one of the most effective ways.^{1,2} In other words, nowadays, utilizing suitable organic tectons with various functional groups that are capable of bridging metal centers to construct such crystalline materials has demonstrated to be an active area of multidisciplinary research, being in connection with crystal engineering, coordination/supramolecular chemistry, and material science.^{2–13}

Among the organic ligands, the versatile multicarboxyl compounds, especially aromatic benzene- and naphthalene-based derivatives, such as benzenedicarboxyl (1,4-,¹⁴ 1,3-,¹⁵ or 1,2-¹⁶), 1,3,5-benzenetricarboxyl,¹⁷ 1,2,4,5-benzenetetracarboxyl,¹⁸ 1,2,3,4,5-benzenepentacarboxyl,¹⁹ and 1,2,3,4,5,6-benzenehexacarboxyl,²⁰ naphthalenedicarboxyl (1,4-²¹ or 2,6-²²), 1,4,5,8-naphthalenetetracarboxyl,²³ have been extensively used in the preparation of a variety of metal-carboxylate complexes owing to their reliable and rich coordination modes.^{14–23} To investigate the influence of the bulky aromatic skeletons of such ligands on the structures and properties of their coordination complexes, anthracene-9-carboxylic acid,²⁴ anthracene-9,10-dicarboxylic acid,²⁵ anthracene-2,3,6,7-tetracarboxylic acid,²⁶ and perylene-3,4,9,10-tetracarboxylic acid²⁷ have been used by us and others to construct a series of coordination metal complexes, which show diverse discrete (dinuclear, tetranuclear, pentanuclear, or hexanuclear) and infinite (1-D, 2-D, or 3-D) structures as well as interesting magnetic and luminescent properties.^{24–27} Despite the remarkable achievements in this aspect,^{1–13} however, to predict and further accurately control the framework array of a given crystalline product still remain a considerable challenge at this stage. This mainly arises from the fact that the subtle assembled progress may be influenced by many intrinsic and external parameters, such as the auxiliary co-ligands,^{1a,f} solvent,^{28a,b} concentration,^{28c,d} counteranion,^{28e} temperature,^{28f} and pH value of the solution,^{28g}

*To whom correspondence should be addressed. Fax: 86-371-63556792. E-mail: chunsenliu@zzuli.edu.cn (C.-S.L.). Fax: 86-22-23766556. E-mail: dumiao@public.tpt.tj.cn (M.D.).

which will determine the formation of different thermodynamically favored crystalline products. For instance, the introduction of 2,2'-bipyridyl-like chelating reagents^{1f} or 4,4'-bipyridyl-like bridging tectons^{1a,c,29} as auxiliary co-ligands, into metal-carboxyl reaction systems will lead to the formation of interesting coordination architectures. In this context, naphthalene-2,3-dicarboxylate (**ndc**) with the extended π -conjugated system, as an analogic but bulky derivative of 1,2-benzenedicarboxylate (**bdc**), has almost not been noticed so far. Significantly, an analysis of the current Cambridge Structural Database (CSD) reveals only one mononuclear Cu^{II} complex [Cu(trpy)(**ndc**)-(H₂O)] with **ndc** and the co-ligand 2,2': 6'2''-terpyridine (trpy).³⁰ Herein, we will describe six new Cd^{II} coordination complexes based on the bulky **ndc** ligand, which display distinct supramolecular architectures under the intervention of chelating or bridging *N*-donor auxiliary co-ligands. Solid-state properties for these crystalline materials, such as fluorescence and thermal stability, have also been investigated.

Experimental Section

Materials and General Methods. With the exception of *trans*-4,4'-azobis(pyridine) (abp), which was prepared according to the literature procedure,³¹ all the starting reagents and solvents for synthesis and analysis were commercially available and used as received. Elemental analyses were performed on a Vario EL III Elementar analyzer. IR spectra were recorded in the range of 4000–400 cm⁻¹ on a Tensor 27 OPUS (Bruker) FT-IR spectrometer with KBr pellets. Thermogravimetric analysis (TGA) experiments were carried out on a Perkin-Elmer Diamond SII thermal analyzer from room temperature to 800 °C under nitrogen atmosphere at a heating rate of 10 °C/min. The emission and excitation spectra were recorded on an F-7000 (Hitachi) spectrophotometer at room temperature.

Synthesis of the Complexes. $[\text{Cd}(\text{ndc})]_{\infty}$ (**1**). A CH₃OH solution (10 mL) of Cd(ClO₄)₂·6H₂O (0.1 mmol) was carefully layered on top of a solution of H₂**ndc** (0.05 mmol) in H₂O (15 mL) in the presence of excess NaOH (0.15 mmol) in a test tube, which was left at room temperature. Colorless sheet single crystals suitable for X-ray analysis appeared at the tube wall after ca. one month. Yield: ca. 40% based on H₂**ndc**. Anal. Calcd for C₁₂H₆CdO₄: C, 44.13; H, 1.85%. Found: C, 43.92; H, 1.94%. IR (cm⁻¹): 3441(m, br), 2972(w), 1823(w), 1556(s), 1471(s), 1407(s), 1351(m), 1273(w), 1232(w), 1206(w), 1145(w), 1090(w), 1045(w), 955(w), 904(w), 870(w), 817(m), 783(w), 742(w), 695(w), 653(w), 589(w), 542(w), 484(w), 451(w).

$\{[\text{Cd}_2(\text{ndc})_2(2\text{bpy})_2(\text{H}_2\text{O})_2](\text{CH}_3\text{OH})_{0.5}\}_2$ (**2**). The same procedure as that for **1** was used with an exception for the introduction of auxiliary co-ligand 2bpy (0.05 mmol). Colorless cubic single crystals suitable for X-ray analysis appeared at the tube wall after ca. three weeks. Yield: ca. 30% based on H₂**ndc**. Anal. Calcd for C_{44.5}H₃₄Cd₂N₄O_{10.5}: C, 52.52; H, 3.37; N, 5.51%. Found: C, 52.79; H, 3.58; N, 5.35%. IR (cm⁻¹): 3443 (w, br), 3053(w), 1602(m), 1565(s), 1472(m), 1443(m), 1397(s), 1362(m), 1316(w), 1249(w), 1210(w), 1179(w), 1152(w), 1114(w), 1060(w), 1016(w), 963(w), 940(w), 897(w), 863(w), 813(m), 764(w), 736(w), 698(w), 649(w), 591(w), 545(w), 479(w).

$[\text{Cd}_2(\text{ndc})_2(\text{phen})_2]_{\infty}$ (**3**). The same procedure as that for **1** was used with an exception for the introduction of auxiliary co-ligand phen (0.05 mmol). Colorless prism single crystals suitable for X-ray analysis appeared at the tube wall after ca. two weeks. Yield: ca. 40% based on H₂**ndc**. Anal. Calcd for C₄₈H₂₈Cd₂N₄O₈: C, 56.88; H, 2.78; N, 5.53%. Found: C, 56.66; H, 2.91; N, 5.64%. IR (cm⁻¹): 3382(w, br), 3053(w), 1958(w), 1825(w), 1625(w), 1591(m), 1550(vs), 1455(m), 1429(w), 1389(s), 1343(m), 1306(w), 1211(w), 1141(w), 1099(w), 1047(w), 987(w), 962(w), 909(w), 849(m), 807(m), 775(m), 725(m), 675(w), 639(w), 615(w), 591(w), 481(w), 419(w).

$\{[\text{Cd}(\text{ndc})(4\text{bpy})_{0.5}(\text{H}_2\text{O})_2](\text{H}_2\text{O})\}_{\infty}$ (**4**). The same procedure as that for **1** was used with an exception for the introduction of auxiliary co-ligand 4bpy (0.05 mmol). Colorless cubic single crystals suitable for X-ray analysis appeared at the tube wall after ca. four

weeks. Yield: ca. 30% based on H₂**ndc**. Anal. Calcd for C₃₄H₃₂-Cd₂N₂O₁₄: C, 44.51; H, 3.52; N, 3.05%. Found: C, 44.63; H, 3.29; N, 2.89%. IR (cm⁻¹): 3390(m, br), 1962(w), 1603(m), 1542(vs), 1467(m), 1395(s), 1225(w), 1141(w), 1107(w), 1068(w), 1044(w), 1014(w), 962(w), 904(w), 860(w), 813(m), 776(w), 690(w), 630(w), 593(w), 536(w), 481(w), 449(w), 419(w).

$\{[\text{Cd}(\text{ndc})(\text{abp})(\text{H}_2\text{O})](\text{H}_2\text{O})\}_{\infty}$ (**5**). The same procedure as that for **1** was used with an exception for the introduction of auxiliary co-ligand abp (0.05 mmol). Wine-colored clubbed single crystals suitable for X-ray analysis appeared at the tube wall after ca. one month. Yield: ca. 40% based on H₂**ndc**. Anal. Calcd for C₂₂H₁₈-CdN₄O₆: C, 48.32; H, 3.32; N, 10.25%. Found: C, 48.55; H, 3.52; N, 10.41%. IR (cm⁻¹): 3422(s, br), 1950(w), 1820(w), 1633(w), 1598(s), 1557(vs), 1472(m), 1453(m), 1408(s), 1317(m), 1228(w), 1141(w), 1090(w), 1062(w), 1007(w), 954(w), 902(w), 847(m), 815(m), 778(w), 746(w), 692(w), 643(w), 593(w), 567(w), 537(w), 488(w), 418(w).

$\{[\text{Cd}(\text{ndc})(\text{bpp})_2](\text{H}_2\text{O})_3\}_{\infty}$ (**6**). The same procedure as that for **1** was used with an exception for the introduction of auxiliary co-ligand bpp (0.05 mmol). Colorless clubbed single crystals suitable for X-ray analysis appeared at the tube wall after ca. three weeks. Yield: ca. 40% based on H₂**ndc**. Anal. Calcd for C₃₈H₄₀CdN₄O₇: C, 58.73; H, 5.19; N, 7.21%. Found: C, 58.89; H, 5.38; N, 7.11%. IR (cm⁻¹): 3407(m, br), 1949(w), 1610(s), 1559(vs), 1503(w), 1469(m), 1450(m), 1425(m), 1395(s), 1357(w), 1224(w), 1143(w), 1070(w), 1047(w), 1015(w), 966(w), 902(w), 862(w), 817(m), 780(w), 757(w), 692(w), 644(w), 609(w), 590(w), 504(w), 418(w).

Caution! Although we have met no problem in handling the cadmium(II) perchlorate during this work, it should be treated cautiously due to the potential explosive nature.

X-ray Data Collection and Structure Determination. X-ray single-crystal diffraction data for complexes **1–6** were collected on a Bruker Smart 1000 CCD area-detector diffractometer with Mo-K α radiation ($\lambda = 0.71073 \text{ \AA}$) by ω scan mode. The program SAINT³² was used for integration of the diffraction profiles. Semi-empirical absorption corrections were applied using SADABS.³³ All the structures were solved by direct methods using the SHELXS program of the SHELXTL package and refined by full-matrix least-squares methods with SHELXL.³⁴ Metal atoms were located from the *E*-maps and the other non-hydrogen atoms were located in successive difference Fourier syntheses and refined with anisotropic thermal parameters on F^2 . The C-bound hydrogen atoms were generated theoretically and refined with isotropic thermal parameters riding on the parent atoms. The hydrogen atoms of the water and partial methanol molecules in **2**, **4**, **5**, and **6** were first located by difference Fourier *E*-maps and then treated isotropically as riding. Further details for structural analysis are summarized in Table 1. Selected bond parameters and H-bonding geometries are listed in Tables S1–S6 (Supporting Information) and Table 2.

Powder X-ray Diffraction. Powder X-ray diffraction (PXRD) patterns of **1–6** were recorded on a Bruker D8 Advance diffractometer (Cu-K α , $\lambda = 1.54056 \text{ \AA}$) at 40 kV and 30 mA, by using a Cu-target tube and a graphite monochromator. The powder samples were prepared by crushing the crystals and the intensity data were recorded by continuous scan in a 2 θ /θ mode from 3° to 80° with a step size of 0.02° and a scan speed of 8°/min. Simulation of the PXRD patterns was carried out by the single-crystal data and diffraction-crystal module of the Mercury (Hg) program.

Results and Discussion

Synthesis Consideration and General Characterization. For a systematic investigation of the coordination features of H₂**ndc**, our strategy is to prepare a series of Cd^{II} complexes by changing systematically the auxiliary co-ligands including the 2,2'-bipyridyl-like chelating ligands (2bpy and phen) or 4,4'-bipyridyl-like bridging ligands with different *N,N'*-donor separations (ca. 7 Å for 4bpy, ca. 9 Å for abp, and ca. 10 Å for bpp). According to our experimental results, when a direct combination of the Cd^{II} salt and organic ligand, that is, using the conventional solution method followed by a solvent evaporation, either no evidence of solid formation or a mass of uncharacterized microcrystalline powders were

Table 1. Crystallographic Data and Structure Refinement Summary for Complexes **1–6**

	1	2	3
empirical formula	C ₁₂ H ₆ CdO ₄	C _{44.5} H ₃₄ Cd ₂ N ₄ O _{10.5}	C ₄₈ H ₂₈ Cd ₂ N ₄ O ₈
formula weight	326.57	1017.56	1013.54
crystal system	monoclinic	triclinic	triclinic
space group	P ₂ 1/c	P ₁	P ₁
a/Å	18.942(2)	13.0727(12)	10.8176(6)
b/Å	7.3043(9)	13.6739(11)	13.6803(6)
c/Å	7.1343(6)	14.0003(13)	14.8358(8)
α/deg	90	70.611(8)	79.974(4)
β/deg	94.013(9)	62.785(9)	83.661(4)
γ/deg	90	78.860(7)	67.607(4)
V/Å ³	984.66(19)	2096.8(3)	1996.62(18)
Z	4	2	2
D/g cm ⁻³	2.203	1.612	1.686
μ/mm ⁻¹	2.215	1.079	1.129
R _{int}	0.0495	0.0375	0.0422
GOF	1.042	1.078	1.026
T/K	294(2)	294(2)	294(2)
R ₁ ^a /wR ₂ ^b [I > 2σ(I)]	0.0274/0.0349	0.0362/0.0702	0.0364/0.0710
ρ _{max} /ρ _{min} (e Å ⁻³)	0.664/-0.877	0.958/-0.363	1.485/-0.710
	4	5	6
empirical formula	C ₃₄ H ₃₂ Cd ₂ N ₂ O ₁₄	C ₂₂ H ₁₈ CdN ₄ O ₆	C ₃₈ H ₄₀ CdN ₄ O ₇
formula weight	917.42	546.80	777.14
crystal system	triclinic	monoclinic	orthorhombic
space group	P ₁	C ₂ /c	P ₂ 1 ₂ 1 ₁
a/Å	7.7519(8)	18.4754(10)	10.4451(6)
b/Å	9.2376(8)	21.5101(14)	12.4548(10)
c/Å	12.0934(10)	12.5984(6)	28.6487(17)
α/deg	80.994(7)	90	90
β/deg	82.035(8)	102.731(5)	90
γ/deg	85.377(8)	90	90
V/Å ³	845.53(13)	4883.6(5)	3727.0(4)
Z	1	8	4
D/g cm ⁻³	1.802	1.487	1.385
μ/mm ⁻¹	1.332	0.937	0.638
R _{int}	0.0308	0.0438	0.0964
GOF	0.943	1.081	0.965
T/K	294(2)	294(2)	294(2)
R ₁ ^a /wR ₂ ^b [I > 2σ(I)]	0.0288/0.0374	0.0285/0.0728	0.0708/0.1739
ρ _{max} /ρ _{min} (e Å ⁻³)	0.330/-0.408	0.726/-0.222	1.520/-1.442

$$^a R_1 = \Sigma(|F_o| - |F_c|)/\Sigma|F_o|. \quad ^b wR_2 = [\Sigma w(|F_o|^2 - |F_c|^2)^2 / \Sigma w(F_o^2)^2]^{1/2}.$$

Table 2. Hydrogen-Bonding Geometry (Å, deg) for **2–4**^a

D–H…A	d(D–H)	d(H…A)	d(D…A)	∠D–H…A
2				
O10–H1W…O8	0.850	2.15	2.966(2)	160
O10–H2W…O3 ^a	0.850	1.88	2.685(1)	156
O9–H3W…O2 ^b	0.850	1.90	2.744(1)	171
O9–H4W…O5 ^c	0.850	2.02	2.861(2)	169
C31–H31A…O1 ^d	0.930	2.42	3.271(1)	153
C38–H38A…O5 ^e	0.930	2.47	3.364(2)	162
3				
C29–H29A…O6 ^a	0.929	2.56	3.341(7)	141
C27–H27A…Cg1 ^b	0.930	3.07	3.916(9)	152
C27–H27A…Cg2 ^c	0.930	3.04	3.904(1)	155
C32–H32A…Cg3 ^d	0.929	2.82	3.649(1)	149
C7–H7A…Cg1 ^e	0.930	2.90	3.656(1)	140
C19–H19A…Cg3 ^f	0.931	3.14	3.775(9)	128
C26–H26A…Cg4 ^g	0.930	3.25	4.011(7)	140
4				
O5–H1W…O2 ^a	0.850	2.08	2.892(1)	161

^a Symmetry codes for **2**: a = -x, -y + 2, -z; b = -x - 1, -y + 2, -z + 1; c = x - 1, y, z + 1; d = -x, -y + 2, -z + 1; e = -x + 1, -y + 2, -z; for **3**: a = x - 1, y, z; b = x - 2, y, z - 1; c = x, y, z - 1; d = -x + 1, -y + 2, -z; e = x + 1, y - 1, z; f = x + 1, y + 1, z; g = -x + 2, -y + 4, -z; (Cg1, Cg2, Cg3, and Cg4 are the centroids of the C14–C16/C21–C23, C16–C21, C2–C4/C9–C11, and C4–C9 phenyl rings in **ndc** ligands of **3**, respectively); for **4**: a = -x + 1, -y, -z.

obtained. Therefore, a properly lowering the reaction speed may facilitate the growth of well-shaped single crystals suitable for X-ray diffraction.³⁵ Considering this point, the synthesis and isolation of **1–6** in this work were carried out through the self-assembly reactions of Cd^{II} salt with H₂**ndc**, together with different auxiliary co-ligands (except in **1**), by using the slow diffusion method under ambient conditions.

Complexes **1–6** are air stable and all general characterizations were carried out by using the single-crystal samples. The IR spectra usually show features attributable to each component of the complexes.³⁶ In the IR spectra of **1–6**, the broad bands centered at ca. 3400 cm⁻¹ (3441 cm⁻¹ for **1**, 3443 cm⁻¹ for **2**, 3382 cm⁻¹ for **3**, 3390 cm⁻¹ for **4**, 3422 cm⁻¹ for **5**, and 3407 cm⁻¹ for **6**) indicate O–H stretching of the aqua molecules. As a matter of fact, the IR absorption of carboxylate group is very complicated due to its coordination diversity. The characteristic bands of the carboxylate groups in **1–6** appear in the usual region at 1610–1542 cm⁻¹ for the antisymmetric stretching vibrations and at 1471–1389 cm⁻¹ for the symmetric stretching vibrations.³⁷ Furthermore, the Δν values [Δν = ν_{asym}(COO⁻) - ν_{sym}(COO⁻)] are 85 and 149 cm⁻¹ for **1**, 168 cm⁻¹ for **2**, 161 cm⁻¹ for **3**, 136 and 147 cm⁻¹ for **4**, 126 and 149 cm⁻¹ for **5**, and 164 and 215 cm⁻¹ for **6**, respectively, which are consistent with their solid structural features as observed in the crystal structures.^{36,37}

Description of the Crystal Structures for **1–6. [Cd(ndc)]_∞** (**1**). Single crystal X-ray diffraction analysis reveals a neutral 2-D layered coordination network of **1**. The asymmetric unit is composed of one Cd^{II} ion and one fully deprotonated **ndc** ligand (see Figure 1a). Each distorted octahedral Cd^{II} center is defined by six carboxylate O atoms from four different **ndc** ligands. All the Cd–O bond distances (2.248(2)–2.407(3) Å) and the bond angles (54.93(9)–141.71(9)°) around Cd^{II} are typical and comparable with those of other similar Cd^{II}–carboxylato complexes in the literature (see Table S1 in the Supporting Information).^{24b,25i,16} In **1**, the **ndc** ligand takes the μ₂-η¹·η²-chelating/bridging coordination mode for each carboxylate (see Scheme 1a and Figure S1 in the Supporting Information). Interestingly, a pair of carboxylate groups (O1–C1–O2 and O3–C12–O4) connects two Cd^{II} centers to form a Cd₂ 14-membered ring subunit with the nonbonding Cd…Cd separation of 5.735(1) Å. These dinuclear subunits are further linked through the monatomic carboxylate bridges to generate a 2-D layer running parallel to the (100) plane (see Figure 1b).

A better insight into the 2-D network of **1** can be achieved by using the topological approach. If one considers each Cd₂ 14-membered ring subunit as a 6-connected node (see Figure 1b), which in turn is connected to six nearest neighbors, then this 2-D layer can be rationalized as a 6-connected 3⁶ topological network (see Figure S2 in the Supporting Information). On the other hand, if both **ndc** ligand and Cd^{II} ion are regarded as the 4-connecting nodes, this structure can be regarded as a familiar 4-connected topological network with the Schläfli symbol of (4⁴.6²) (see Figure 1c). Notably, all 4-connecting nodes in this case take the tetrahedral geometries and thus, result in a nonplanar feature of the 2-D layer.

{[Cd₂(ndc)₂(2bpy)₂(H₂O)₂](CH₃OH)_{0.5}}₂ (**2**). When the bidentate chelating ligand 2bpy was introduced into the assembled system, a distinct centrosymmetric tetranuclear complex **2** was produced (see Figure 2). The asymmetric unit contains two crystallographically unique Cd^{II} ions (Cd1 and

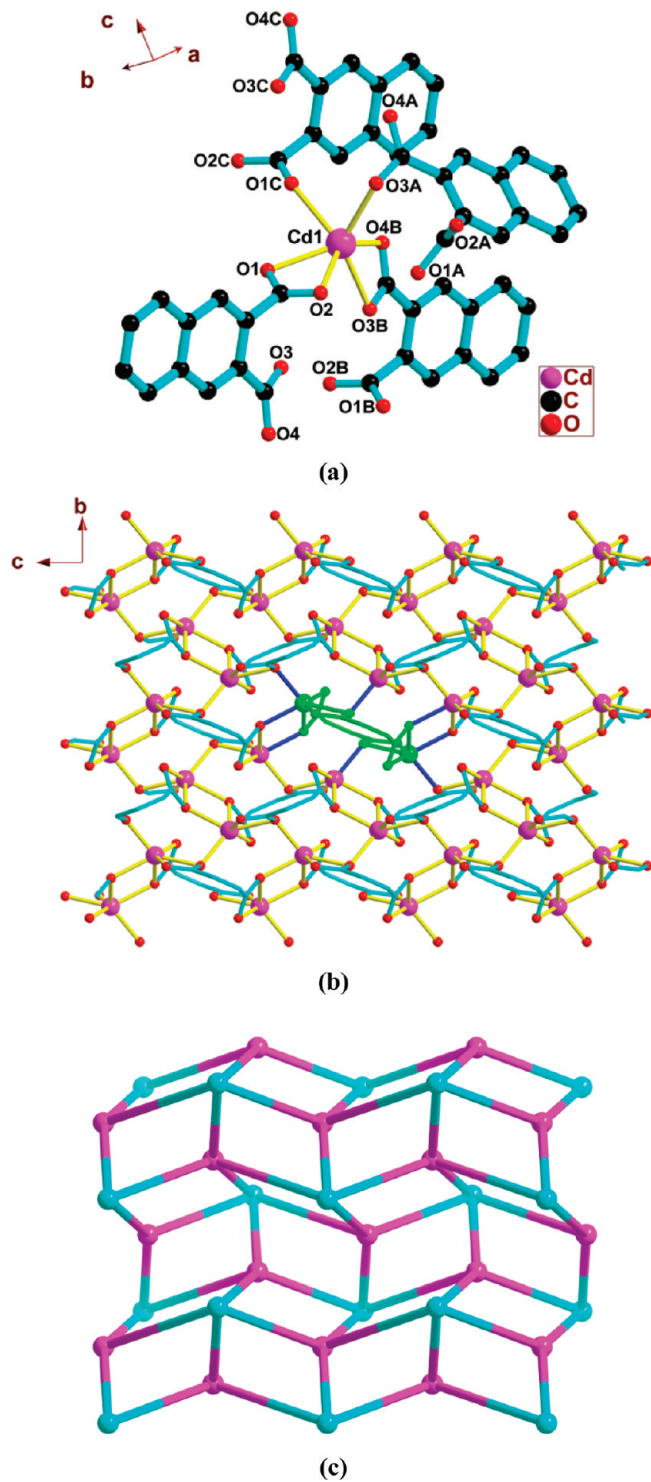
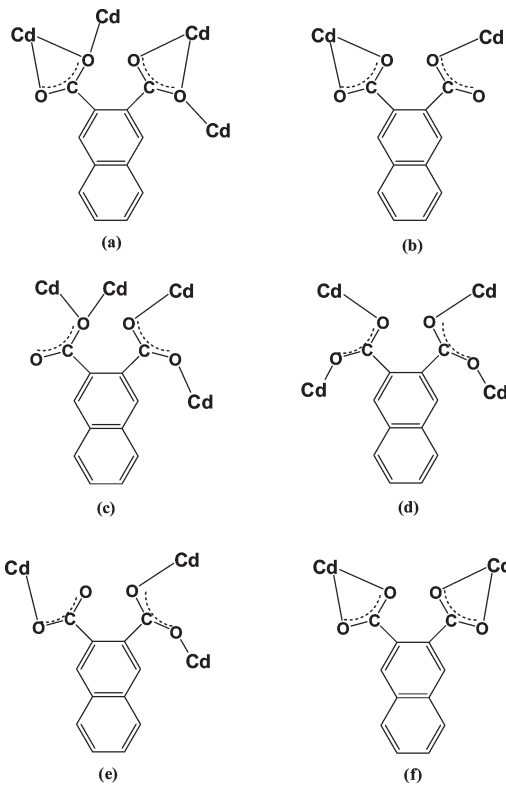


Figure 1. Views of 1. (a) Local coordination environment of Cd^{II} ($A = -x + 1, y - 1/2, -z + 1/2$; $B = -x + 1, -y + 2, -z$; $C = -x + 1, -y + 2, -z + 1$). (b) 2-D coordination layer, in which one Cd₂ 14-membered ring subunit and its connectivity are highlighted in green and blue (partial ndc ligands were omitted for clarity). (c) Schematic representation of the 4-connected (4⁴.6²) topology (pink spheres: Cd^{II} nodes; cyan spheres: ndc ligands).

Cd²⁺, two ndc ligands, two chelating 2bpy ligands, two H₂O ligands, and half a lattice CH₃OH molecule (see Figure 2a). The Cd^{II} ion is penta-coordinated by two N-donors from one 2bpy ligand (Cd^{II}–N1 = 2.351(4) Å; Cd^{II}–N2 = 2.312(4) Å; N1–Cd^{II}–N2 = 70.32(15)°) and three O atoms from two different ndc ligands as well as one H₂O ligand. Several

Scheme 1. Coordination modes of ndc in 1–6^a



^a(a) for 1: $\mu_2\text{-}\eta^1\text{:}\eta^2$ -chelating/bridging mode for both carboxylate groups of ndc; (b) for 2: $\mu_1\text{-}\eta^1\text{:}\eta^1$ -chelating mode (left) and $\mu_1\text{-}\eta^1\text{:}\eta^0$ -monodentate mode (right) for the carboxylate groups of ndc; (c) and (d) for 3: $\mu_2\text{-}\eta^2\text{:}\eta^0$ -monodentate-bridging mode (left) and $\mu_2\text{-}\eta^1\text{:}\eta^1$ -syn-anti bridging mode (right) for the carboxylate groups of ndc in (c) as well as $\mu_2\text{-}\eta^1\text{:}\eta^1$ -syn-anti bridging mode for both carboxylate groups of ndc in (d); (e) for 4: $\mu_1\text{-}\eta^1\text{:}\eta^0$ -monodentate mode (left) and $\mu_2\text{-}\eta^1\text{:}\eta^1$ -syn-anti bridging mode (right) for the carboxylate groups of ndc; (f) for 5 and 6: $\mu_1\text{-}\eta^1\text{:}\eta^1$ -chelating mode for both carboxylate groups of ndc.

parameters are used to define the geometry of penta-coordinated metal centers, and the most common one is the τ factor defined by Addison et al. ($\tau = 0$ for a regular square-pyramid and $\tau = 1$ for a regular trigonal-bipyramidal).³⁸ The τ value of 0.04 for Cd^{II} indicates a nearly ideal square-pyramid environment. The Cd^{II} ion takes a distorted pentagonal-dipyramidal geometry via coordinating to two N-donors from one 2bpy ligand (Cd^{II}–N3 = 2.314(4) Å; Cd^{II}–N4 = 2.3364 Å; N3–Cd^{II}–N4 = 70.21(16)°) and five O atoms from two ndc ligands and one H₂O ligand. All the Cd–O (2.183(3)–2.620(3) Å) and Cd–N (2.312(4) and 2.351(4) Å) bond lengths as well as the bond angles around Cd^{II} (52.75(11)–154.28(12)°) (see Table S2 in the Supporting Information) are in the normal range expected for similar complexes.^{24b,25i,16} For ndc ligand, two different kinds of carboxylate groups exist, namely, $\mu_1\text{-}\eta^1\text{:}\eta^1$ -chelating fashion for O3–C12–O4 and O5–C13–O6 and $\mu_1\text{-}\eta^1\text{:}\eta^0$ -monodentate mode for O1–C1–O2 and O7–C24–O8 (see Scheme 1b and Figure S3 in the Supporting Information). Intramolecular O–H···O interactions (see Figure 2a) are observed between the coordinated H₂O (O10) and carboxylate O3/O8 atoms of ndc (O10–H1W···O8 and O10–H2W···O3; see Table 2 for detailed hydrogen-bonding geometry).³⁹

In addition, the adjacent tetranuclear units are extended into a 1-D chain (see Figure 2b) along the [10 $\bar{1}$] direction by intermolecular O–H···O bonds (O9–H3W···O2 and O9–H4W···O5; see Table 2). Moreover, a 2-D layer running

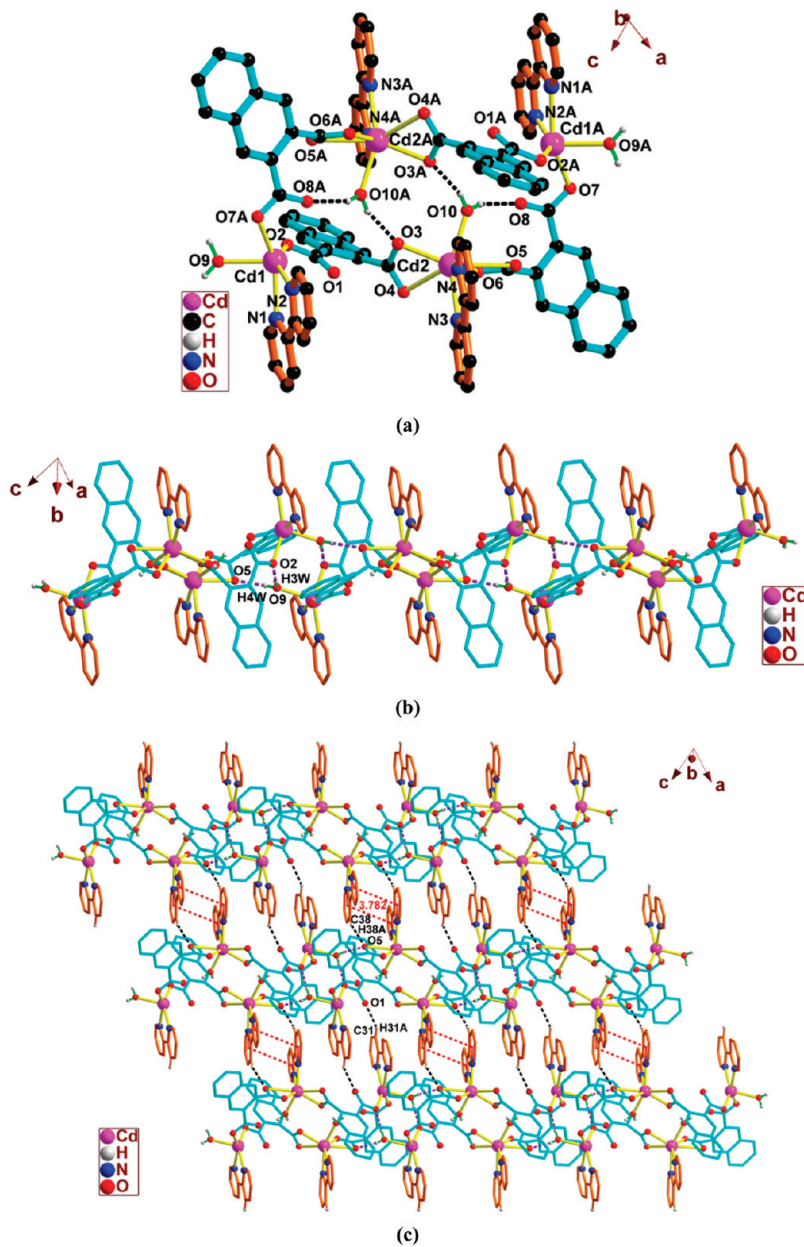


Figure 2. Views of 2. (a) Local coordination environments of Cd^{II} showing the intramolecular $\text{O}-\text{H}\cdots\text{O}$ interactions (black dashed lines) ($A = -x, -y + 2, -z$). (b) 1-D chain formed by the intermolecular $\text{O}-\text{H}\cdots\text{O}$ H-bonding (purple dashed lines). (c) 2-D layer formed by the coeffects of the intermolecular $\text{C}-\text{H}\cdots\text{O}$ (black dashed lines) and $\pi\cdots\pi$ stacking (red dashed lines) interactions.

parallel to the (010) plane is constructed (see Figure 2c), by intermolecular $\text{C}-\text{H}\cdots\text{O}$ interactions between 2bpy and **ndc** ($\text{C}31-\text{H}31\text{A}\cdots\text{O}1$ and $\text{C}38-\text{H}38\text{A}\cdots\text{O}5$; see Table 2) as well as $\pi\cdots\pi$ stacking between the 2bpy ligands.⁴⁰ The centroid–centroid and interplanar separations are 3.782 and 3.448 Å with their dihedral angle of 3.0°. This structure also contains various intra- and internetwork $\text{C}-\text{H}\cdots\pi$ supramolecular interactions between the naphthyl and/or pyridyl rings of **ndc** and 2bpy ligands with an edge-to-face orientation, further affording an overall 3-D supramolecular network ($d = 2.875, 2.897, 3.091$, and 3.014 \AA , $A = 136, 142, 123$, and 145° ; d and A stand for $\text{H}\cdots\pi$ separations and $\text{C}-\text{H}\cdots\pi$ angles in the $\text{C}-\text{H}\cdots\pi$ patterns, respectively),⁴¹ as calculated by the PLATON program.⁴²

[$\text{Cd}_2(\text{ndc})_2(\text{phen})_2]_{\infty}$ (**3**). Sequentially, when we used phen instead of 2bpy as the chelating co-ligand, a 1-D coordination polymer **3** was produced (see Figure 3). The asymmetric

unit contains two crystallographically unique Cd^{II} ions (Cd1 and Cd2), two fully deprotonated **ndc** ligands, and two phen ligands. Each Cd^{II} center is in a distorted octahedral geometry (see Table S3 in the Supporting Information), being surrounded by four carboxylate O atoms from three **ndc** ligands and two N-donors from one phen (see Figure 3a). However, the Cd1 and Cd2 centers have slight difference in bond distances and angles (i.e., $\text{Cd}1-\text{N}1 = 2.401(3)$ Å, $\text{Cd}1-\text{N}2 = 2.384(4)$ Å, and $\text{N}1-\text{Cd}1-\text{N}2 = 70.19(13)^\circ$; $\text{Cd}2-\text{N}3 = 2.410(4)$ Å, $\text{Cd}2-\text{N}4 = 2.395(4)$ Å, and $\text{N}3-\text{Cd}2-\text{N}4 = 68.61(15)^\circ$). Still, all the Cd–O and Cd–N distances and bond angles around each Cd^{II} fall into the normal range (see Table S3 in the Supporting Information). Two different coordination modes of the carboxylate groups are observed for the **ndc** ligands in **3**, namely, $\mu_2\text{-}\eta^2\text{:}\eta^0$ -monodentate-bridging mode for $\text{O}1-\text{C}1-\text{O}2$ and $\mu_2\text{-}\eta^1\text{:}\eta^1$ -*syn-anti* bridging mode for $\text{O}3-\text{C}12-\text{O}4$, $\text{O}5-\text{C}13-\text{O}6$,

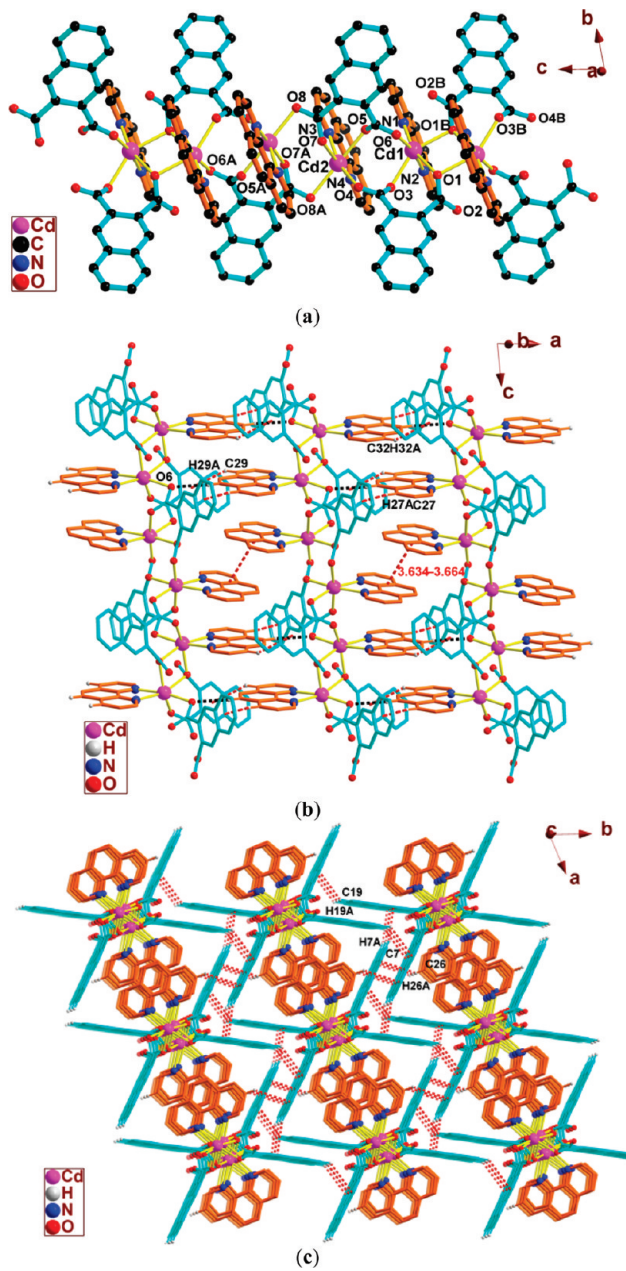


Figure 3. Views of 3. (a) 1-D motif along [001] showing the local coordination environments of Cd^{II} ($A = -x + 2, -y + 2, -z$; $B = -x + 2, -y + 2, -z + 1$). (b) 2-D layer formed by the coeffects of intermolecular $\text{C}-\text{H}\cdots\text{O}$ (black dashed lines), $\text{C}-\text{H}\cdots\pi$ (red dashed lines), and $\pi\cdots\pi$ stacking (red dashed lines) interactions. (c) 3-D network viewed along the c axis, formed by interlayer $\text{C}-\text{H}\cdots\pi$ interactions.

and $\text{O}7-\text{C}24-\text{O}8$ (see Scheme 1c,d and Figure S4 in the Supporting Information). The dihedral angles between the carboxylate planes and the naphthyl ring skeletons in **ndc** ligands are in the range of $29.1\text{--}48.0^\circ$. As a result, the $\text{Cd}1$ and $\text{Cd}2$ ions are in turn connected by three $\mu_2\text{-}\eta^1\text{:}\eta^1\text{-syn-anti}$ carboxylate groups of two different **ndc** ligands ($\text{O}3-\text{C}12-\text{O}4$, $\text{O}5-\text{C}13-\text{O}6$, and $\text{O}7-\text{C}24-\text{O}8$) to form two nonplanar eight-membered rings composed of $\text{Cd}1-\text{O}3-\text{C}12-\text{O}4-\text{Cd}2-\text{O}5-\text{C}13-\text{O}6$ and $\text{Cd}2-\text{O}7-\text{C}24-\text{O}8-\text{Cd}2\text{A}-\text{O}7\text{A}-\text{C}24\text{A}-\text{O}8\text{A}$, with the nonbonding $\text{Cd}1\cdots\text{Cd}2$ and $\text{Cd}2\cdots\text{Cd}2\text{A}$ separations of $4.0034(5)$ and $4.1451(6)$ Å, respectively (see Figure 3a). As such, two symmetry-related $\text{O}1-\text{C}1-\text{O}2$ carboxylate groups link two adjacent $\text{Cd}1$ ions to

generate a planar four-membered ring of $\text{Cd}1-\text{O}1-\text{Cd}1\text{B}-\text{O}1\text{B}$ with the nonbonding $\text{Cd}1\cdots\text{Cd}1\text{B}$ separation of $3.6205(5)$ Å (see Figure 3a). As a consequence, a 1-D chain is formed along the [001] direction. In addition, the adjacent 1-D chains are further linked to generate a 2-D sheet running parallel to the (010) plane (see Figure 3b), and then an overall 3-D network (see Figure 3c), by the coeffects of interlayer $\pi\cdots\pi$ stacking between the parallel phenyl and/or pyridyl of phen in an offset fashion with the centroid-centroid and interplanar separations of $3.379\text{--}3.386$ Å and $3.3791\text{--}3.3862$ Å,⁴⁰ as well as $\text{C}-\text{H}\cdots\text{O}$ interactions between the phenyl rings of phen and carboxylates of **ndc** ($\text{C}29-\text{H}29\text{A}\cdots\text{O}6$; see Table 2)³⁹ and $\text{C}-\text{H}\cdots\pi$ interactions between phen and **ndc** with an edge-to-face orientation ($d = 2.821\text{--}3.250$ Å; $A = 128\text{--}155^\circ$ in the $\text{C}-\text{H}\cdots\pi$ patterns).⁴¹

$\{[\text{Cd}(\text{ndc})(4\text{bpy})_{0.5}(\text{H}_2\text{O})_2](\text{H}_2\text{O})\}_{\infty}$ (**4**). When 4bpy, a rigidly linear bridging co-ligand, was used instead of the chelating ligand 2bpy or phen, a 2-D layered network **4** was obtained (see Figure 4 as well as Table S4 and Figures S5–S7 in the Supporting Information). The asymmetric unit is composed of one Cd^{II} ion, one **ndc** ligand, half a 4bpy ligand, two H_2O ligands, and one lattice H_2O molecule. The coordination geometry around each Cd^{II} can be best described as a distorted octahedron defined by three carboxylate O atoms from different **ndc** ligands, two H_2O ligands, and one N-atom donor from one 4bpy (see Figure 4a). For the **ndc** ligand, two types of coordination modes are found for the carboxylate groups, that is, $\mu_1\text{-}\eta^1\text{:}\eta^0$ -monodentate mode for $\text{O}1-\text{C}1-\text{O}2$ and $\mu_2\text{-}\eta^1\text{:}\eta^1\text{-syn-anti}$ bridging mode for $\text{O}3-\text{C}12-\text{O}4$ (see Scheme 1e and Figure S5 in the Supporting Information). Thus, the adjacent Cd^{II} ions are connected to form a 1-D chain motif along the [100] direction with the intrachain nonbonding $\text{Cd}\cdots\text{Cd}$ separations of $5.377(4)$ and $4.815(8)$ Å (see Figure S6 in the Supporting Information). The adjacent 1-D motifs are further assembled into a 2-D layered network along the (010) plane, in virtue of the bridging 4bpy ligands with the $\text{Cd}\cdots\text{Cd}$ separation of $11.725(5)$ Å (see Figure 4b). In addition, such 2-D layers are extended into an overall 3-D network (see Figure 4c) by interlayer $\text{O}5-\text{H}1\text{W}\cdots\text{O}2$ interactions between the water ligands and carboxylates (see Table 2 for details).

From the viewpoint of network topology, the 2-D coordination layer has a (3,4)-connected $(4^2.6)(4^2.6^3.8)$ pattern, in which the **ndc** ligand can be regarded as the 3-connected node to bridge three Cd^{II} ions and each Cd^{II} as a 4-connected node by linking to three **ndc** and one Cd^{II} via 4bpy (see Figure S7 in the Supporting Information). However, if the interlayer $\text{O}5-\text{H}1\text{W}\cdots\text{O}2$ hydrogen bonds are also considered, the **ndc** ligands and Cd^{II} ions can be regarded as the 4- and 5-connected nodes, respectively. In this way, the resulting binodal (4,5)-connected 3-D hydrogen-bonded network has the Schläfli symbol of $(4^4.6^2)(4^4.6^4.8^2)$ (see Figure 4d).

$\{[\text{Cd}(\text{ndc})(\text{abp})(\text{H}_2\text{O})](\text{H}_2\text{O})\}_{\infty}$ (**5**). To explore the effect of the relevant 4,4'-bipyridyl-like spacers on the construction of Cd –**ndc** coordination networks, a semirigidly dipyrindyl ligand abp with a rich π -conjugated system was used, affording a 3-D coordination framework **5** (see Figure 5). The fundamental building unit contains one Cd^{II} ion, one fully deprotonated **ndc** ligand, one abp ligand, one water ligand, and one lattice water molecule (see Table S5 in the Supporting Information). The $\text{Cd}1$ center is located in a distorted pentagonal-dipyramidal geometry, via coordinating to one N-donor of abp and four O atoms of two **ndc** ligands in the

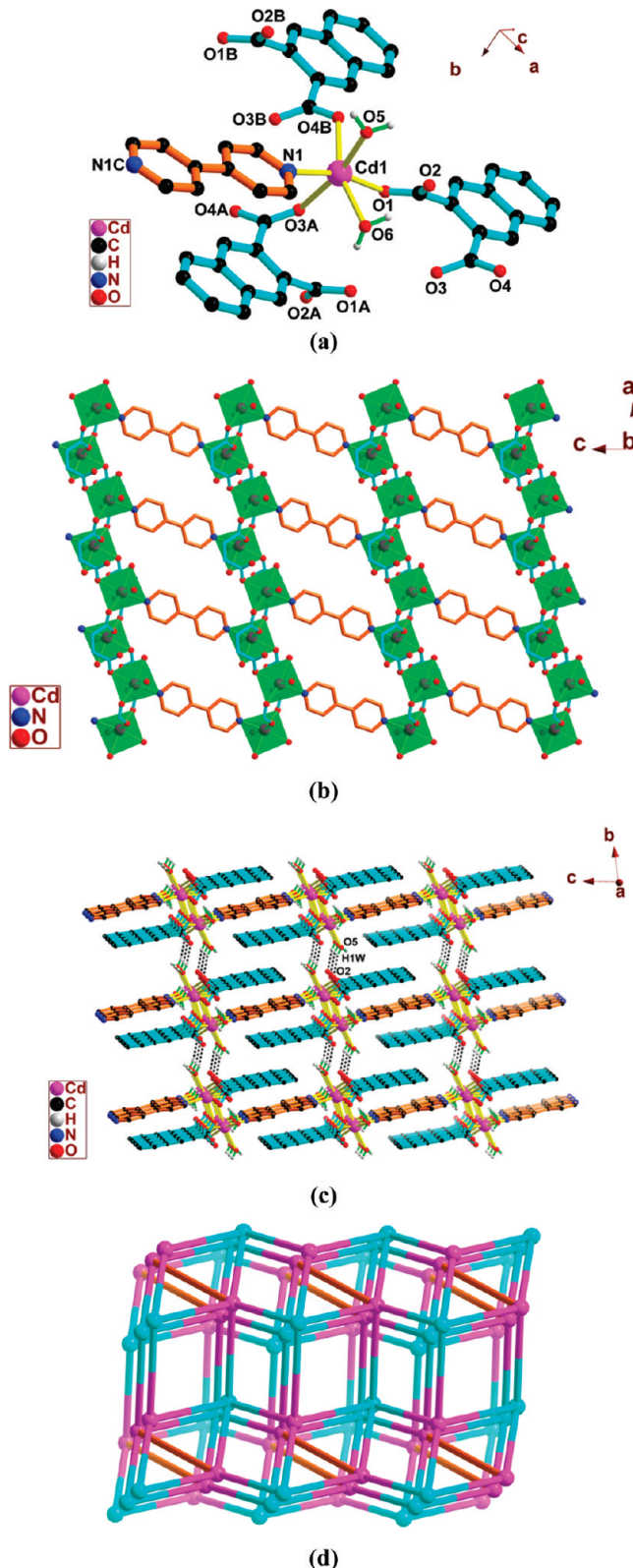


Figure 4. Views of 4. (a) Local coordination environment of Cd^{II} ($A = -x + 1, -y + 1, -z$; $B = x - 1, y, z$; $C = -x, -y + 1, -z - 1$). (b) 2-D coordination layer (partial carbon atoms of naphthalimide in **nDC** were omitted for clarity), (c) 3-D supramolecular framework viewed along the [100] direction, constructed by the interlayer $\text{O}-\text{H}\cdots\text{O}$ interactions (black dashed lines) between the water ligands and the uncoordinated carboxylate O atoms of the **nDC** ligands. (d) Schematic representation of the (4,5)-connected $(4^4.6^2)(4^4.6^4.8^2)$ 3-D topology (pink spheres: Cd^{II} ; cyan spheres: **nDC**; orange rods: 4bpy).

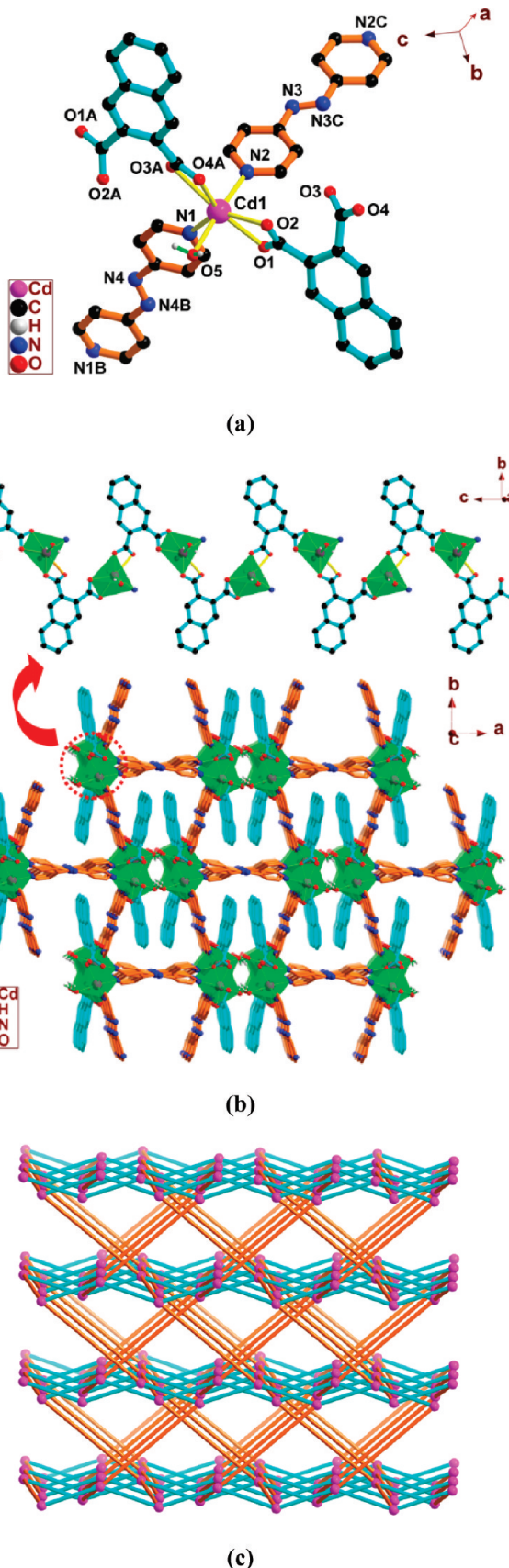


Figure 5. Views of 5. (a) Local coordination environment of Cd^{II} ($A = x, -y + 1, z + 1/2$; $B = -x + 1/2, -y + 1/2, -z + 2$; $C = -x + 1, -y + 1, -z + 1$). (b) 3-D coordination network viewed along the c axis, highlighting the $\text{Cd}-\text{nDC}$ 1-D chain along [001]. (c) Schematic representation of the 3-D 4-connected **irl** ($4^2.6^3.8$) topology (pink spheres: Cd^{II} ; cyan rods: **nDC**; orange rods: abp).

equatorial plane as well as one water ligand and another abp at the axial sites with the O5–Cd1–N2 angle of 173.51(10)° (see Figure 5a). In **5**, each tetradentate **ndc** ligand bridges two adjacent Cd^{II} ions with the $\mu_1\eta^1:\eta^1$ -chelating mode of carboxylate (see Scheme 1f and Figure S8 in the Supporting Information) to give rise to a 1-D zigzag chain along the [001] direction (see Figure 5b, top). Such staggered 1-D arrays are further interlinked via the abp ligands along different crystallographic directions, to finally produce a 3-D coordination network (see Figure 5b, bottom).

Analysis of network topology provides a convenient tool in designing and understanding the complicated crystal structures such as coordination polymers or hydrogen-bonded networks.³ Such structures can usually be reduced to simple topological networks with different connectivity of the components. To further demonstrate the 3-D structure of **5**, we can consider each Cd^{II} center as a nonplanar 4-connecting node, which is linked to four equivalent nodes through two **ndc** and two abp spacers (see Figure 5c). As a result, an unusual uninodal 4-connected **irl** net with (4².6³.8) topology is formed,³ instead of the familiar 4-connecting nets with the tetrahedral and/or square-planar nodes, such as diamond (or **dia**),^{43a,b} CdSO₄ (or **cds**) (6⁵.8),^{43c,d} NbO (6⁴.8²),^{43e,f} pts (4².8⁴),^{43g,h} lvt (4².8⁴),^{43i,j} SrAl₂ (or **sra**) (4².6³.8),^{43k,l} moganite (4².6².8²)(4.6⁴.8)₂,^{43m,n} and quartz dual (or “dense” 7⁵.9),^{43o}

$\{[\text{Cd}(\text{ndc})(\text{bpp})_2](\text{H}_2\text{O})_3\}_{\infty}$ (**6**). A 3-D chiral coordination framework **6** was isolated, when we used a flexible 4,4'-bipyridyl-like molecule bpp with a longer *N,N'*-donor separation of ca. 10 Å, which crystallizes in space group *P*2₁2₁2₁ (see Figure 6 as well as Figures S9 and S10 in the Supporting Information). The asymmetric unit contains one Cd^{II} ion, one **ndc** ligand, two bpp ligands, and three lattice water molecules. Each Cd^{II} center is seven-coordinated in a distorted pentagonal-dipyramidal geometry, being defined by one N-donor of bpp (Cd1–N4: 2.351(8) Å) and four O atoms of two **ndc** ligands (Cd1–O: 2.349(6)–2.499(8) Å) in the equatorial plane as well as two N atoms from the other two bpp ligands (Cd1–N1: 2.349(9) Å; Cd1–N3B: 2.352(10) Å) at the axial sites with the N1–Cd1–N3B angle of 176.3(4)° (see Figure 5a). Similar to **5**, each **ndc** ligand in **6** also adopts the $\mu_1\eta^1:\eta^1$ -chelating mode for carboxylate (see Scheme 1f and Figure S9 in the Supporting Information), and the bpp ligand serves as a head-to-end spacer.

The most attractive structural feature in **6** is the chiral 3-D coordination framework with the flack parameter of 0.04(6).⁴⁴ The chiral unit in **6** can be considered as a pair of right- and left-handed 2_1 helical chains, running perpendicularly along the [100] and [010] directions (see Figures 6b and S10 in the Supporting Information). The left-handed 2_1 helix $[-\text{Cd}-\text{ndc}-]_n$ along the *a* axis with a screw pitch of 10.46(9) Å, are decorated with the bpp ligands at two sides as arms (Figure 6b right and Figure S10 left in the Supporting Information). And the right-handed 2_1 helix $[-\text{Cd}-\text{bpp}-]_n$ along the *b* axis with a screw pitch of 12.35(9) Å mainly originates from the flexible and twisted configuration of the bpp ligands (Figure 6b left and Figure S10 right in the Supporting Information). As is known, helical structural motifs generally have an axial chirality⁴⁵ and the extension of such helical motifs into a 3-D homochiral lattice requires the suitable homochiral discriminative interactions.⁴⁶ In the reported examples for homochiral coordination architectures, the 1-D helical coordination arrays^{46a,b} normally

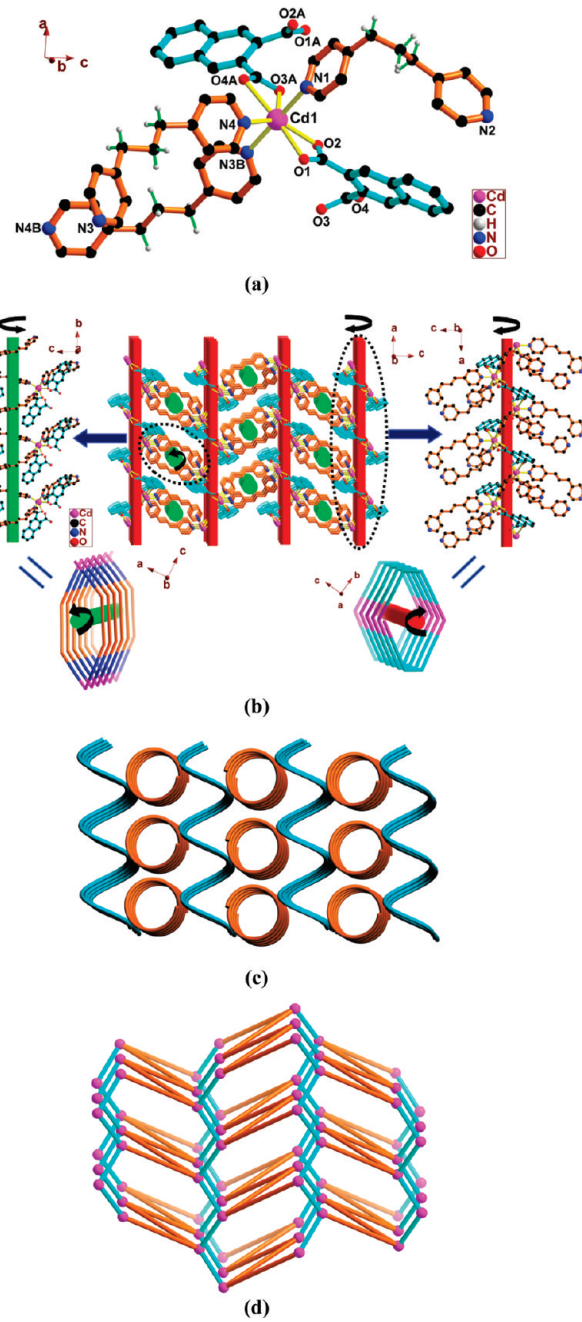


Figure 6. Views of **6**. (a) Local coordination environment of Cd^{II} ($A = x + 1/2, -y + 5/2, -z + 2$; $B = -x + 1, y + 1/2, -z + 3/2$). (b) A detailed illustration of the 3-D homochiral coordination framework (middle), constructed by alternate left-handed (red bars) and right-handed (green bars) helical motifs. (c) Schematic representation of the left- and right-handed helices arranged perpendicularly. (d) Schematic representation of the 3-D 4-connected diamond (**dia**) topology (pink spheres: Cd^{II}; cyan rods: **ndc**; orange rods: bpp).

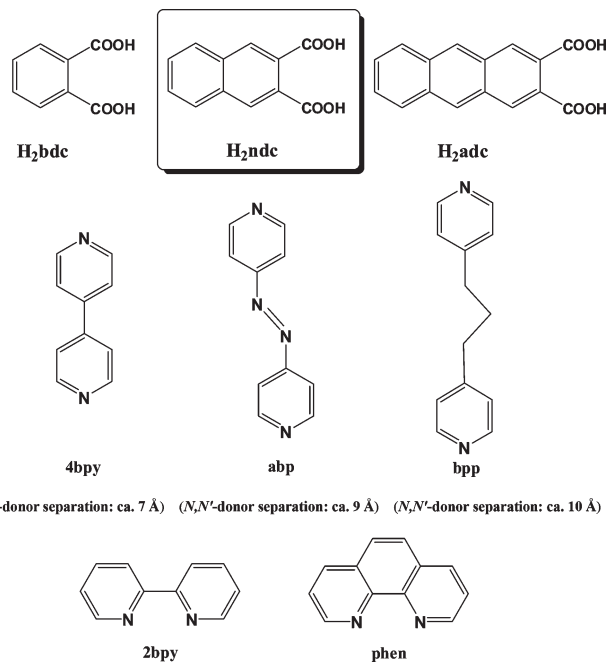
homochirally aggregate via weaker intermolecular contacts, such as $\pi \cdots \pi$ stacking,^{46c} C–H \cdots π /C–H \cdots N,^{46d} C–H \cdots Cl,^{46e} and argentophilic interactions.^{46f} However, in this case, the alternate right- and left-handed helices are further linked by Cd1–O/N coordination bonds to afford a 3-D homochiral coordination network (see Figure 6b, middle, Figure 6c, and Figure S10, middle in the Supporting Information). That is, such interactions can also be used to transmit the local chiral information into the resulting 3-D homochiral assembly. From the viewpoint of network

topology, the 3-D structure of **6** can be reduced as a classical 4-connected diamond (**dia**) lattice by considering Cd^{II} ions as the 4-connected nodes and all ligands as the 2-connected spacers (see Figure 6d).^{3e-g}

Structural Diversity of 1–6. Structural transformation and diversification are evidently observed in the present series of mixed-ligand coordination complexes, and their structural difference can be mainly ascribed to the choice of different *N*-donor auxiliary co-ligands. As described above, the initial complex [Cd(**ndc**)]_∞ (**1**) shows a 2-D (4⁴.6²) coordination network. It has been known that the chelating 2bpy terminal will have a great influence on structural assembly of metal–carboxylate systems, which can usually reduce the structural dimensionality of such coordination networks by occupying the metal binding sites.^{1f} Here, when 2bpy was applied as the auxiliary co-ligand, a discrete tetranuclear complex **2** was obtained. Similarly, phen that has a larger conjugated backbone will also terminate the metal coordination sites and result in lower-dimensional coordination arrays.^{1a,25f} On the other hand, the bulky aromatic backbone of phen may affect the spatial arrangement of the bridging **ndc** ligand and facilitate the formation of π···π stacking and C–H···π interactions, which can extend the low-dimensional coordination motifs into higher-dimensional supramolecular frameworks.^{25f} As a result, when we used phen instead of 2bpy, a 1-D coordination polymer **3** that is completely different from **2** was obtained. The 4,4'-bipyridyl-like bridging ligands with different *N,N'*-donor separations modified by the spacers, such as 4bpy (*N,N'*-donor separation: ca. 7 Å), abp (*N,N'*-donor separation: ca. 9 Å), and bpp (*N,N'*-donor separation: ca. 10 Å), have dissimilar skeleton rigidity and steric effects on the direction of unexpected coordination solids.²⁹ In this regard, to further evaluate their roles on adjusting the Cd–**ndc** crystalline networks, complexes **4–6** were prepared, showing a 2-D (3,4)-connected (4².6)(4².6³.8) layer, a 3-D uninodal network with the rare **irl** (4².6³.8) topology, and a 3-D homochiral diamond (**dia**) framework, respectively. From the viewpoint of crystal engineering, we can temporarily conclude that the structural discrepancy in the resulting coordination complexes should originate from the intervention of different *N*-donor auxiliary co-ligands even though their crystalline lattices cannot be accurately forecasted at present.

Effect of the Bulky Naphthalene Skeleton of H₂ndc on Structural Assembly. As typical aromatic carboxyl ligands, benzene-based dicarboxylic acids,^{14–16} especially benzene-1,2-dicarboxylic acid¹⁶ (**H₂bdc**, see Chart 1) have been widely employed to construct diverse coordination architectures. However, the rational use of their closely related naphthalene-based dicarboxyl analogues, such as naphthalene-2,3-dicarboxylic acid (**H₂ndc**) with a larger π-conjugated system and the bulky aromatic skeleton, has been less explored to date.³⁰ From the above discussion of crystal structures, it can be seen that, in comparison with **H₂bdc**, the **H₂ndc** ligand has two obvious characteristics: (1) the electronic nature of its extended π-conjugated system and the steric hindrance of the bulky naphthalene ring that may affect the coordination modes of carboxylate, and thus, determine the final coordination arrays; (2) the extended π-conjugated system that normally results in C–H···π and/or π···π stacking interactions from the viewpoint of the electronic nature, along with the increased overlap of the aromatic surface areas, play an important role in forming the final supramolecular

Chart 1



lattices, namely, extending the low-dimensional coordination entities into higher-dimensional supramolecular networks. These characteristics allow **H₂ndc** to show different building functions comparing with its benzene-based analogue **H₂bdc**. For instance, two different 2-D photoluminescent complexes [Cd(**bdc**)(H₂O)]_∞^{16d,n,p,q} and [Cd(**bdc**)]_∞^{16m} have been reported. The former exhibits a 2-D honeycomb-like network constructed from the [CdO₇] single helical chains linked by corner-sharing oxygen atoms of the **bdc** ligands, which adopt the μ₂-η¹:η²-chelating/bridging and μ₃-η¹:η²-bridging coordination modes for the two carboxylate groups. The latter has a 2-D square grid network with seven-coordinated Cd^{II} centers as well as μ₂-η¹:η²-chelating/bridging and μ₃-η²:η²-bridging/chelating binding modes for the two carboxylate groups of **bdc**. When **H₂bdc** is replaced by **H₂ndc** in this work, a new 2-D complex [Cd(**ndc**)]_∞ (**1**) is formed but with the distorted octahedral six-coordinated Cd^{II} centers and the μ₂-η¹:η²-chelating/bridging coordination mode for each carboxylate group of **ndc** (see Figure S1 in the Supporting Infoamtion). Also, a 1-D coordination polymer {[Cd(**bdc**)(2bpy)(H₂O)]_∞} incorporating 2bpy as the auxiliary co-ligand, has been known.^{16h,j} In contrast, the structure of **2** involving **ndc** and 2bpy in this work shows a distinct discrete tetranuclear motif {[Cd₂(**ndc**)₂(2bpy)₂(H₂O)₂](CH₃OH)_{0.5}}. As such, we have noticed that a discrete dinuclear complex [Cd₂(**bdc**)₂(phen)₄](H₂O)₄^{16l} and a 1-D species {[Cd(**bdc**)(phen)(H₂O)]_∞}^{16j} have been documented with the six-coordinated Cd^{II} centers as well as μ₁-η¹:η¹-chelating and μ₁-η¹:η⁰-monodentate coordination modes for carboxylates of **bdc**. However, when we used **H₂ndc** to react with Cd^{II} in the presence of phen, a 1-D coordination polymer [Cd₂(**ndc**)₂(phen)₂]_∞ (**3**) was isolated with different μ₂-η²:η⁰-monodentate-bridging and μ₂-η¹:η¹-syn-anti bridging coordination modes for carboxylates of **ndc** (see Figure S4 in the Supporting Information). In addition, {[Cd(**bdc**)(4bpy)(H₂O)]_∞}^{16o} with a 2-D (4,4) network and {[Cd(H₂bdc)₂(4bpy)]_∞}^{16k} with a 3-D homochiral framework have also been prepared, which both adopt μ₁-η¹:η⁰-monodentate coordination mode for each carboxylate group in **bdc**.

In this context, the related Cd^{II} complex $\{[\text{Cd}(\text{ndc})(4\text{bpy})_{0.5}(\text{H}_2\text{O})_2](\text{H}_2\text{O})\}_{\infty}$ (**4**) with **ndc** and 4bpy co-ligand shows a 2-D (3,4)-connected (4².6)(4².6³.8) layered network with mixed $\mu_1\text{-}\eta^1\text{:}\eta^0$ -monodentate and $\mu_2\text{-}\eta^1\text{:}\eta^1$ -syn-anti bridging coordination modes for the carboxylate groups of **ndc** (see Figure S5 in the Supporting Information). That is, although the available binding sites of H₂**ndc** and H₂**bdc** are very similar, their coordination chemistry and the role for involving supramolecular interactions are different that should be ascribed to the electronic nature of its extended π -conjugated system and the bulk skeleton of naphthalene of **ndc**. This work, therefore, offers an opportunity to make a potential comparison of the corresponding coordination complexes constructed from two structurally related naphthalene- and benzene-based dicarboxylate tectons. And further, from the viewpoint of ligand design, the present finding may provide an effective method for the design and preparation of new coordination architectures, just by changing the aromatic skeletons of different polycarboxyl systems.

Photoluminescence Properties. Metal–organic coordination complexes constructed from d¹⁰ metal centers and conjugated organic ligands are promising candidates for hybrid photoactive materials with potential applications such as light-emitting diodes (LEDs).^{47,48} These crystalline solids usually show regulatable photoluminescent properties and high thermal stability.⁴⁸ Thus, solid-state emission spectra of the as-synthesized Cd^{II} complexes **1–6** have been investigated at room temperature (see Figure S11 in the Supporting Information). Excitation of the microcrystalline samples of **1–6** at 349, 341, 358, 364, 375, and 336 nm produces the intense luminescence with the peak maxima at 371, 361, 424, 427, 416, and 361 nm, respectively. To further analyze the nature of these emission bands, the photoluminescent properties of H₂**ndc** and auxiliary co-ligands 2bpy, phen, 4bpy, abp, and bpp have also been investigated under the same experimental conditions (see Figure S12 in the Supporting Information). By comparing the locations and profiles of their excitation/emission peaks with those of complexes **1–6**, we can presume that these emissions are neither metal-to-ligand charge transfer (MLCT) nor ligand-to-metal charge transfer (LMCT) in nature, because the Cd^{II} ion with d¹⁰ configuration is difficult to oxidize or to reduce²⁶ and should mainly be ascribed to the intraligand $\pi \rightarrow \pi^*$ transitions arising from the **ndc** ligand, namely, ligand-to-ligand charge transfer (LLCT).^{48c} The results are similar to those of the related Cd^{II} complexes with the naphthalene-based carboxyl ligands.^{24b} In addition, the different emissions in **2–6** may result from the auxiliary N-donor co-ligands. In comparison with the emission peaks of free H₂**ndc**, the enhancement and red shift of the luminescence emissions in **3–5** or the blue shift in **1, 2**, and **6** may be due to the chelating and/or bridging effect of the deprotonated **ndc** ligands, which effectively increases or decreases the rigidity and conjugation upon metal coordination, and then affects the loss of energy via a radiationless pathway of the intraligand ($\pi \rightarrow \pi^*$) excited state.^{48c} Further, the additional peak in the range of 450–500 nm for **5** is very weak and should be ascribed to background.

Generally, the greater the extent of the π -electron system (i.e., degree of conjugation), the lower the energy of the low-lying $\pi \rightarrow \pi^*$ transition, which, consequently, leads to a shift of the absorption and fluorescence spectra to longer wavelengths. Comparing the emission of benzene-1,2-dicarboxylic acid (H₂**bdc**) (peak maxima at 345 nm) with that of

H₂**ndc** here,^{16k,n} it can be seen that the bathochromic shift of the maxima emission peak of H₂**ndc** ($\lambda_{\text{max}} = 397$ nm; $\lambda_{\text{ex}} = 368$ nm) should be mainly related to the extended π -conjugated system. As such, we noticed that the observed emissions related to a series of Cd^{II}–**bdc** complexes with or without the different chelating or bridging N-donor co-ligands would be probably assigned to the intraligand fluorescent emission and/or ligand-to-metal charge transfer (LMCT).^{16a,b,d,f,g,k,m,n} The different emission bands of the relevant complexes (Cd^{II}–**ndc** vs Cd^{II}–**bdc**) may be due to the significant difference of their supramolecular structures with benzene- or naphthalene-based dicarboxylate ligands because the fluorescence behaviors are closely associated with the metal ions and the nature of the ligands coordinated around them.⁴⁷

Thermal Stability of 1–6. Thermogravimetric analysis (TGA) experiments were conducted to examine the thermal stability of **1–6**. As shown in Figure S13 in the Supporting Information, complex **1** remains intact until heating to 380 °C, and then suffers two consecutive weight losses that end at 640 °C (peaking at 430 and 514 °C). Further heating to 800 °C reveals no weight loss and the final solid holds a weight of 14.16% of the total sample. For **2**, the TGA curve suggests the first weight loss of 4.98% in the range of 50–230 °C, corresponding to a gradual removal of methanol guests (calcd: 1.57%) and water ligands (calcd: 3.54%). The host framework starts to decompose beyond 250 °C in three consecutive steps of weight loss (peaking at 278, 393, and 606 °C), which does not stop until heating to 800 °C. Complex **3** is thermally stable upon heating to ca. 250 °C followed by three stages of weight loss peaking at 308, 342, and 669 °C. The weight loss of 76.12% observed from 250 to 700 °C is very close to the calculated value of 77.82%, corresponding to the exclusion of phen and **ndc** ligands. With regard to **4**, the initial weight loss of 12.15% in the TGA curve from 30 to 75 °C (peaking at 58 °C) suggests the release of lattice and coordination water molecules (calcd: 11.79%). With that, the residual framework remains largely unchanged until the decomposition onsets at 240 °C with three consecutive steps of weight loss, followed by a slow weight loss not ending until 800 °C. The critical weight loss (17.35%) in the range of 240–280 °C (peaking at 262 °C) can be ascribed to the loss of 4bpy ligands (calcd: 17.02%), showing the collapse of the 2-D coordination framework. The other two peaks (388 and 529 °C) in the TGA curve also reveal the weight loss processes of the residual components. The TGA trace of **5** indicates that the first weight loss occurs in the temperature range of 50–140 °C (peaking at 98 °C), which can be ascribed to the expulsion of lattice and coordinated water molecules (calcd: 6.60%; found: 6.86%). Then, a series of complicated weight losses occur above 140 °C (peaking at 202, 258, 378, and 573 °C), indicating collapse of the residual framework. Further heating to 800 °C only reveals a continuous and slow weight loss. As for the TGA curve of **6**, the first weight loss of 7.21% appears in 70–180 °C (peaking at 161 °C), corresponding to the loss of lattice water molecules (calcd: 6.96%). The following three-step weight loss of ca. 79.36% in 180–600 °C can be attributed to the elimination of bpp and **ndc** (calcd: 78.58%). The residue gradually decomposes upon further heating until 800 °C. Similar to the cases of Cd^{II} benzene-1,2-dicarboxylate (**bdc**) complexes,¹⁶ the volatility of coordinated or lattice water molecules from host frameworks is commonly observed at low temperatures (<200 °C), which can further lead to a decomposition of

the coordination structures. In addition, degradation of the organic components of **1–6** (see Figure S13 in the Supporting Information) and Cd^{II}-**bdc** complexes^{16a,g,k,m,n} similarly starts in the temperature range of 150–350 °C, resulting in pyrolysis of the as-synthesized solid materials.

PXRD Results. To confirm whether the crystal structures of **1–6** are truly representative of the bulk materials, powder X-ray diffraction (PXRD) experiments have been carried out. The experimental and simulated PXRD patterns of the corresponding complexes are shown in Figure S14 in the Supporting Information. Although the experimental patterns have a few unindexed diffraction lines and some peaks are slightly broadened in comparison with those simulated from the single crystal data, it can still be considered that the bulk synthesized materials and the as-grown crystals are homogeneous for **1–6**.

Conclusions

We have succeeded in obtaining a series of Cd^{II} coordination architectures showing discrete tetranuclear motif as well as infinite 1-D, 2-D, and 3-D frameworks with a bulky naphthalene-based dicarboxylate (**ndc**), sometimes incorporating different auxiliary N-donor co-ligands. With the exception of such auxiliary chelating or bridging co-ligands, the results reveal that the naphthalene ring skeleton in **ndc** showing the extended π-conjugated system and steric bulk may play an important role in the formation of **1–6**, in comparison with those based on the structurally related **bdc** tecton. In addition, complexes **1–6** show blue fluorescent emissions at room temperature, mainly owing to the bulk naphthalene ring of **ndc**. Accordingly, our present findings will further enrich the crystal engineering strategy and offer the possibility of controlling the formation of the desired network structures. Following this lead, this work will prompt us to achieve more functional crystalline solids via such a reliable synthetic route, by using the analogous bulky aromatic dicarboxyl ligands with larger π-conjugated systems, such as anthracene-2,3-dicarboxylic acid (H₂**adc**, see Chart 1). Further efforts on this project are underway in our laboratory.

Acknowledgment. This work was supported by the National Natural Science Fund of China (Grant Nos. 20801049 and 20771095), the Startup Fund for Ph.D.s of Natural Scientific Research of Zhengzhou University of Light Industry (Grant No. 2007BSJJ001 to C.S.L.), Henan Outstanding Youth Science Fund (to C.S.L.), and Tianjin Normal University (to M.D.).

Supporting Information Available: Crystallographic information files (CIFs) of **1–6**, additional structural figures for **1–6** (Figures S1–S10), solid-state excitation/emission spectra of **1–6** (Figure S11) and the free ligands (Figure S12), TGA plots of **1–6** (Figure S13), and PXRD patterns for **1–6** (Figure S14), as well as tables of selected bond parameters for **1–6** (Tables S1–S6). This material is available free of charge via the Internet at <http://pubs.acs.org>.

References

- (1) For recent reviews please see (a) Leininger, S.; Olenyuk, B.; Stang, P. J. *Chem. Rev.* **2000**, *100*, 853. (b) Moulton, B.; Zaworotko, M. J. *Chem. Rev.* **2001**, *101*, 1629. (c) Yaghi, O. M.; O'Keeffe, M.; Ockwig, N. W.; Chae, H. K.; Eddaoudi, M.; Kim, J. *Nature* **2003**, *423*, 705. (d) Janiak, C. *Dalton Trans.* **2003**, 2781. (e) Kitagawa, S.; Kitaura, R.; Noro, S. *Angew. Chem., Int. Ed.* **2004**, *43*, 2334. (f) Ye, B.-H.; Tong, M.-L.; Chen, X.-M. *Coord. Chem. Rev.* **2005**, *249*, 545. (g) Steel, P. J. *Acc. Chem. Res.* **2005**, *38*, 243. (h) Robin, A. Y.; Fromm, K. M. *Coord. Chem. Rev.* **2006**, *250*, 2127. (i) Champness, N. R. *Dalton Trans.* **2006**, 877. (j) Hong, M. *Cryst. Growth Des.* **2007**, *7*, 10. (k) Robson, R. *Dalton Trans.* **2008**, 5113. (l) O'Keeffe, M. *Chem. Soc. Rev.* **2009**, *38*, 1215. (m) Qiu, S.; Zhu, G. *Coord. Chem. Rev.* **2009**, *293*, 2891. (n) Liang, H.; He, Y.; Ye, Y.; Xu, X.; Cheng, F.; Sun, W.; Shao, X.; Wang, Y.; Li, J.; Wu, K. *Coord. Chem. Rev.* **2009**, *293*, 2959.
- (2) For example: (a) Fujita, M.; Fujita, N.; Ogura, K.; Yamaguchik, K. *Nature* **1999**, *400*, 52. (b) Wang, Q.-M.; Mak, T. C. W. *J. Am. Chem. Soc.* **2001**, *123*, 7594. (c) Campos-Fernández, C. S.; Schottel, B. L.; Chifotides, H. T.; Bera, J. K.; Bacsa, J.; Koomen, J. M.; Russell, D. H.; Dunbar, K. R. *J. Am. Chem. Soc.* **2005**, *127*, 12909. (d) Argent, S. P.; Adams, H.; Riis-Johannessen, T.; Jeffery, J. C.; Harding, L. P.; Ward, M. D. *J. Am. Chem. Soc.* **2006**, *128*, 72. (e) Wang, P.; Ma, J.-P.; Dong, Y.-B.; Huang, R.-Q. *J. Am. Chem. Soc.* **2007**, *129*, 10620. (f) Hou, J.-Z.; Li, M.; Li, Z.; Zhan, S.-Z.; Huang, X.-C.; Li, D. *Angew. Chem., Int. Ed.* **2008**, *47*, 1711. (g) Jiang, H.-L.; Liu, B.; Akita, T.; Haruta, M.; Sakurai, H.; Xu, Q. *J. Am. Chem. Soc.* **2009**, *131*, 11302.
- (3) Wells, A. F. *Three-Dimensional Nets and Polyhedra*; Wiley-Interscience: New York, 1977. (b) Wells, A. F. *Further Studies of Three-Dimensional Nets*; ACA Monograph No. 8, American Crystallographic Association: Buffalo, NY, 1979. (c) O'Keeffe, M.; Hyde, B. G. *Crystal Structures I. Patterns and Symmetry*; Mineralogical Society of America: Washington, DC, 1996. (d) Barnett, S. A.; Champness, N. R. *Coord. Chem. Rev.* **2003**, *246*, 145. (e) Carlucci, L.; Ciani, G.; Proserpio, D. M. *Coord. Chem. Rev.* **2003**, *246*, 247. (f) Batten, S. R.; Neville, S. M.; Turner, D. R. *Coordination Polymers: Design, Analysis and Application*; Royal Society of Chemistry (RSC) Publishing: Cambridge, 2008. (g) O'Keeffe, M.; Peskov, M. A.; Ramsden, S. J.; Yaghi, O. M. *Acc. Chem. Res.* **2008**, *41*, 1782 and the associated website <http://rscr.anu.edu.au/>. (h) Kostakis, G. E.; Powell, A. K. *Coord. Chem. Rev.* **2009**, *293*, 2686.
- (4) For example: (a) Yam, V. W. W.; Lo, K. K.-W.; Fung, W. K.-M.; Wang, C.-R. *Coord. Chem. Rev.* **1998**, *171*, 17. (b) Swavey, S.; Swavey, R. *Coord. Chem. Rev.* **2009**, *293*, 2627. (c) Zou, R.-Q.; Zhong, R.-Q.; Du, M.; Pandey, D. S.; Xu, Q. *Cryst. Growth Des.* **2008**, *8*, 452.
- (5) For example: (a) Miller, J. S.; Drilon, M. *Magnetism: Molecules to Materials*; Wiley-VCH: Weinheim, Germany, 2002. (b) Wernsdorfer, W.; Aliaga-Alcalde, N.; Hendrickson, D. N.; Christou, G. *Nature* **2002**, *416*, 406. (c) Konar, S.; Mukherjee, P. S.; Zangrando, E.; Lloret, F.; Chaudhuri, N. R. *Angew. Chem., Int. Ed.* **2002**, *41*, 1561. (d) Wang, X.-Y.; Wang, Z.-M.; Gao, S. *Chem. Commun.* **2008**, 281. (e) Zeng, Y.-F.; Hu, X.; Liu, F.-C.; Bu, X.-H. *Chem. Soc. Rev.* **2009**, *38*, 469.
- (6) For example: (a) Seo, J. S.; Whang, D.; Lee, H.; Jun, S. I.; Oh, J.; Jeon, Y. J.; Kim, K. *Nature* **2000**, *404*, 982. (b) Zou, R.-Q.; Sakurai, H.; Han, S.; Zhong, R.-Q.; Xu, Q. *J. Am. Chem. Soc.* **2007**, *129*, 8402.
- (7) For example: (a) Chen, B.; Eddaoudi, M.; Hyde, S. T.; O'Keeffe, M.; Yaghi, O. M. *Science* **2001**, *291*, 1021. (b) Kitaura, R.; Kitagawa, S.; Kubota, Y.; Kobayashi, T. C.; Kindo, K.; Mita, Y.; Matsuo, A.; Kobayashi, M.; Chang, H. C.; Ozawa, T. C.; Suzuki, M.; Sakata, M.; Takata, M. *Science* **2002**, *298*, 2358. (c) Bradshaw, D. T.; Prior, T. J.; Cussen, E. J.; Claridge, J. B.; Rosseinsky, M. J. *J. Am. Chem. Soc.* **2004**, *126*, 6106. (d) Lin, X.; Blake, A. J.; Wilson, C.; Sun, X. Z.; Champness, N. R.; George, M. W.; Hubberstey, P.; Mokaya, R.; Schröder, M. *J. Am. Chem. Soc.* **2006**, *128*, 10745. (e) Li, J.-R.; Kuppler, R. J.; Zhou, H.-C. *Chem. Soc. Rev.* **2009**, *38*, 1477.
- (8) For example: (a) Mitzi, D. B.; Wang, S.; Field, C. A.; Chess, C. A.; Guloy, A. M. *Science* **1995**, *267*, 1473. (b) Su, W.-P.; Hong, M.; Weng, J.-B.; Cao, R.; Lu, S.-F. *Angew. Chem., Int. Ed.* **2000**, *39*, 2911. (c) Zheng, S.-L.; Zhang, J.-P.; Wong, W.-T.; Chen, X.-M. *J. Am. Chem. Soc.* **2003**, *125*, 6882. (d) Coronado, E.; Day, P. *Chem. Rev.* **2004**, *104*, 5419.
- (9) For examples: (a) Kesani, B.; Lin, W. *Coord. Chem. Rev.* **2003**, *246*, 305. (b) Hou, H.; Wei, Y.; Song, Y.; Mi, L.; Tang, M.; Li, L.; Fan, Y. *Angew. Chem., Int. Ed.* **2005**, *44*, 6067. (c) Innocenzi, P.; Lebeau, B. *J. Mater. Chem.* **2005**, *15*, 3821. (d) Cariati, E.; Macchi, R.; Roberto, D.; Ugo, R.; Galli, S.; Casati, N.; Macchi, P.; Sironi, A.; Bogani, L.; Caneschi, A.; Gatteschi, D. *J. Am. Chem. Soc.* **2007**, *129*, 9410.
- (10) For example: (a) James, S. L. *Chem. Soc. Rev.* **2003**, *32*, 276. (b) Zhao, J.; Mi, L.; Hu, J.; Hou, H.; Fan, Y. *J. Am. Chem. Soc.* **2008**, *130*, 15222.
- (11) For example: (a) Iglesias, R.; Marcos, M.; Serrano, J. L.; Sierra, T.; Pérez-Jubindo, M. A. *Chem. Mater.* **1996**, *8*, 2611. (b) Okubo, T.; Kawajiri, R.; Mitani, T.; Shimoda, T. *J. Am. Chem. Soc.* **2005**, *127*, 17598. (c) Bujak, M.; Angel, R. J. *J. Solid State Chem.* **2005**, *178*, 2237. (d) Zhang, W.; Ye, H.-Y.; Xiong, R.-G. *Coord. Chem. Rev.* **2009**, *293*, 2980.
- (12) Chen, W.; Yuan, H. M.; Wang, J. Y.; Liu, Z. Y.; Xu, J. J.; Yang, M.; Chen, J. S. *J. Am. Chem. Soc.* **2003**, *125*, 9266.

- (13) For example: (a) Gütlich, P.; Hauser, A.; Spiering, H. *Angew. Chem., Int. Ed.* **1994**, *33*, 2024. (b) Kahn, O.; Martinez, C. J. *Science* **1998**, *279*, 44.
- (14) For example: (a) Li, H.; Eddaoudi, M.; O'Keeffe, M.; Yaghi, O. M. *Nature* **1999**, *402*, 276. (b) Hafizovic, J.; Bjorgen, M.; Olsbye, U.; Dietzel, P. D. C.; Bordiga, S.; Prestipino, C.; Lamberti, C.; Lillerud, K. P. *J. Am. Chem. Soc.* **2007**, *129*, 3612. (c) Wang, G.-H.; Li, Z.-G.; Jia, H.-Q.; Hu, N.-H.; Xu, J.-W. *Cryst. Growth Des.* **2008**, *8*, 1932. (d) Wang, F.-K.; Yang, S.-Y.; Huang, R.-B.; Zheng, L.-S.; Batten, S. R. *CrystEngComm* **2008**, *10*, 1211. (e) Prajapati, R.; Mishra, L.; Kimura, K.; Raghavaiah, P. *Polyhedron* **2009**, *28*, 600.
- (15) For example: (a) Rosi, N. L.; Kim, J.; Eddaoudi, M.; Chen, B.; O'Keeffe, M.; Yaghi, O. M. *J. Am. Chem. Soc.* **2005**, *127*, 1504. (b) Chen, P.-K.; Che, Y.-X.; Zheng, J.-M.; Batten, S. R. *Chem. Mater.* **2007**, *19*, 2162. (c) Zhang, L.; Qin, Y.-Y.; Li, Z.-J.; Lin, Q.-P.; Cheng, J.-K.; Zhang, J.; Yao, Y.-G. *Inorg. Chem.* **2008**, *47*, 8286. (d) Chun, H.; Jung, H.; Seo, J. *Inorg. Chem.* **2009**, *48*, 2043. (e) Habib, H. A.; Hoffmann, A.; Hoppe, H. A.; Janiak, C. *Discuss. Faraday Soc.* **2009**, *174*, 1742.
- (16) (a) Wang, L.-Y.; Yang, Y.; Liu, K.; Li, B.-L.; Zhang, Y. *Cryst. Growth Des.* **2008**, *8*, 3902. (b) Hu, T.-L.; Zou, R.-Q.; Li, J.-R.; Bu, X.-H. *Dalton Trans.* **2008**, *1302*. (c) Zhang, W.-L.; Liu, Y.-Y.; Ma, J.-F.; Jiang, H.; Yang, J. *Polyhedron* **2008**, *27*, 3351. (d) Luo, F.; Che, Y.-X.; Zheng, J.-M. *J. Coord. Chem.* **2008**, *61*, 2097. (e) Guo, F.; Yu, W.; Zhang, X.-L. *Chin. J. Struct. Chem.* **2008**, *27*, 1123. (f) Wang, X.-L.; Bi, Y.-F.; Lin, H.-Y.; Liu, G.-C. *Cryst. Growth Des.* **2007**, *7*, 1086. (g) Du, M.; Jiang, X.-J.; Zhao, X.-J. *Inorg. Chem.* **2007**, *46*, 3984. (h) Wang, X.-Y.; Dong, C.-C.; Deng, X.-T.; Wang, C.-G.; Hu, B. *Acta Crystallogr.* **2007**, *E63*, m2079. (i) Cui, Y.-C.; Wang, J.-J.; Che, G.-B.; Li, C.-B. *Acta Crystallogr.* **2006**, *E62*, m2761. (j) Thirumurugan, A.; Rao, C. N. R. *J. Mater. Chem.* **2005**, *15*, 3852. (k) Wang, X.; Qin, C.; Wang, E.; Xu, L. *J. Mol. Struct.* **2005**, *737*, 49. (l) Sun, Y.-G.; Gao, E.-J.; Wei, D.-Z.; Liu, Y.-N. *Chin. J. Struct. Chem.* **2005**, *24*, 1298. (m) Tang, Y.-Z.; Qian, S.-S.; Wang, X.-S.; Zhao, H.; Huang, X.-F.; Li, Y.-H.; Jiao, X.-C.; Xiong, R.-G. *Z. Anorg. Allg. Chem.* **2004**, *630*, 1623. (n) Wang, S.; Hou, Y.; Wang, E.; Li, Y.; Xu, L.; Peng, J.; Liu, S.; Hu, C. *New J. Chem.* **2003**, *27*, 1144. (o) Suresh, E.; Boopalan, K.; Jasra, R. V.; Bhadhrade, M. M. *Inorg. Chem.* **2001**, *40*, 4078. (p) Vaz, J. L. L.; Duc, G.; Petit-Ramel, M.; Faure, R.; Vittori, O. *Can. J. Chem.* **1996**, *74*, 359. (q) Robl, C. Z. *Anorg. Allg. Chem.* **1988**, *566*, 144.
- (17) For example: (a) Chui, S. S.-Y.; Lo, S. M.-F.; Charmant, J. P. H.; Orpen, A. G.; Williams, I. D. *Science* **1999**, *283*, 1148. (b) Eddaoudi, M.; Li, H.; Yaghi, O. M. *J. Am. Chem. Soc.* **2000**, *122*, 1391. (c) Zhang, J.; Chen, Y.-B.; Chen, S.-M.; Li, Z.-J.; Cheng, J.-K.; Yao, Y.-G. *Inorg. Chem.* **2006**, *45*, 3161. (d) Yang, E.-C.; Liu, Z.-Y.; Wang, X.-G.; Batten, S. R.; Zhao, X.-J. *CrystEngComm* **2008**, *10*, 1140. (e) Fang, Q.; Zhu, G.; Xue, M.; Wang, Z.; Sun, J.; Qiu, S. *Cryst. Growth Des.* **2008**, *8*, 319.
- (18) For example: (a) Braverman, M. A.; LaDuka, R. L. *CrystEngComm* **2008**, *10*, 117. (b) Li, M.-X.; Miao, Z.-X.; Shao, M.; Liang, S.-W.; Zhu, S.-R. *Inorg. Chem.* **2008**, *47*, 4481. (c) Lin, J.-D.; Cheng, J.-W.; Du, S.-W. *Cryst. Growth Des.* **2008**, *8*, 3345. (d) Qi, Y.; Che, Y. X.; Luo, F.; Batten, S. R.; Liu, Y.; Zheng, J. M. *Cryst. Growth Des.* **2008**, *8*, 1654. (e) Liu, X.-G.; Wang, L.-Y.; Zhu, X.; Li, B.-L.; Zhang, Y. *Cryst. Growth Des.* **2009**, *9*, 3997. (f) Chowdhuri, D. S.; Rana, A.; Bera, M.; Zangrando, E.; Dalai, S. *Polyhedron* **2009**, *28*, 2131. (g) Yao, J.; Wu, L.; Li, Y.; Mei, X. J. *Chem. Cryst.* **2009**, *39*, 246.
- (19) (a) Wang, J.; Lin, Z.; Ou, Y.-C.; Yang, N.-L.; Zhang, Y.-H.; Tong, M.-L. *Inorg. Chem.* **2008**, *47*, 190. (b) Wang, X.-Y.; Sevov, S. C. *Inorg. Chem.* **2008**, *47*, 1037.
- (20) Fox example: (a) Chui, S. S.-Y.; Siu, A.; Feng, X.; Zhang, Z.-Y.; Mak, T. C. W.; Williams, I. D. *Inorg. Chem. Commun.* **2001**, *4*, 467. (b) Kumagai, H.; Oka, Y.; Akita-Tanaka, M.; Inoue, K. *Inorg. Chim. Acta* **2002**, *332*, 176. (c) Zhao, M.-G.; Shi, J.-M.; Liu, C.-Q.; Xu, W.; Chen, Y.-Q. *Pol. J. Chem.* **2003**, *77*, 829. (d) Yang, E.; Zhang, J.; Li, Z.-J.; Gao, S.; Kang, Y.; Chen, Y.-B.; Wen, Y.-H.; Yao, Y.-G. *Inorg. Chem.* **2004**, *43*, 6525.
- (21) For example: (a) Bickley, J. F.; Bonar-Law, R. P.; Femoni, C.; MacLean, E. J.; Steiner, A.; Teat, S. J. *J. Chem. Soc., Dalton Trans.* **2000**, *4025*. (b) Lu, J. Y.; Schauss, V. *CrystEngComm* **2002**, *4*, 623. (c) Zheng, X.-J.; Jin, L.-P.; Gao, S.; Lu, S.-Z. *New J. Chem.* **2005**, *29*, 798. (d) Maji, T. K.; Ohba, M.; Kitagawa, S. *Inorg. Chem.* **2005**, *44*, 9225. (e) Chun, H.; Dybtsev, D. N.; Kim, H.; Kim, K. *Chem.—Eur. J.* **2005**, *11*, 3521. (f) Yang, J.; Yue, Q.; Li, G.-D.; Cao, J.-J.; Li, G.-H.; Chen, J.-S. *Inorg. Chem.* **2006**, *45*, 2857.
- (22) For example: (a) Eddaoudi, M.; Kim, J.; Vodak, D.; Sudik, A.; Wachter, J.; O'Keeffe, M.; Yaghi, O. M. *Proc. Nat. Acad. Sci. U. S. A.* **2002**, *99*, 4900. (b) Choi, E.-Y.; Park, K.; Yang, C.-M.; Kim, H.; Son, J.-H.; Lee, S. W.; Lee, Y. H.; Min, D.; Kwon, Y.-U. *Chem.—Eur. J.* **2004**, *10*, 5535. (c) Dinca, M.; Long, J. R. *J. Am. Chem. Soc.* **2005**, *127*, 9376. (d) Zhu, H.-F.; Fan, J.; Okamura, T.; Sun, W.-Y.; Ueyama, N. *Cryst. Growth Des.* **2005**, *5*, 289. (e) Serre, C.; Mellot-Draznieks, C.; Surble, S.; Audebrand, N.; Filinchuk, Y.; Ferey, G. *Science* **2007**, *315*, 1828.
- (23) For example: (a) Zhao, X.-J.; Tao, J. *Appl. Organomet. Chem.* **2004**, *18*, 491. (b) Chen, L.-F.; Zhang, J.; Song, L.-J.; Ju, Z.-F. *Inorg. Chem. Commun.* **2005**, *8*, 555. (c) Wang, P.; Moorefield, C. N.; Panzer, M.; Newkome, G. R. *Chem. Commun.* **2005**, *4405*. (d) Nielsen, R. K. B.; Kongshaug, K. O.; Fjellvag, H. *Solid State Sci.* **2006**, *8*, 1237. (e) Kerbellec, N.; Daiguebonne, C.; Bernot, K.; Guillou, O.; Guillou, X. L. *J. Alloys Compd.* **2008**, *451*, 377.
- (24) (a) Liu, C.-S.; Wang, J.-J.; Yan, L.-F.; Chang, Z.; Bu, X.-H.; Sañudo, E. C.; Ribas, J. *Inorg. Chem.* **2007**, *46*, 6299. (b) Liu, C.-S.; Shi, X.-S.; Li, J.-R.; Wang, J.-J.; Bu, X.-H. *Cryst. Growth Des.* **2006**, *6*, 656. (c) Liu, C.-S.; Chen, P.-Q.; Chang, Z.; Wang, J.-J.; Yan, L.-F.; Sun, H.-W.; Bu, X.-H.; Lin, Z.; Li, Z.-M.; Batten, S. R. *Inorg. Chem. Commun.* **2008**, *11*, 159. (d) Liu, C.-S.; Sañudo, E. C.; Yan, L.-F.; Chang, Z.; Wang, J.-J.; Hu, T.-L. *Transition Met. Chem.* **2009**, *34*, 51.
- (25) (a) Tanaka, D.; Horike, S.; Kitagawa, S.; Ohba, M.; Hasegawa, M.; Ozawa, Y.; Toriumi, K. *Chem. Commun.* **2007**, *3142*. (b) Uemura, T.; Ono, Y.; Kitagawa, K.; Kitagawa, S. *Macromolecules* **2008**, *41*, 87. (c) Ma, S.; Wang, X.-S.; Collier, C. D.; Manis, E. S.; Zhou, H.-C. *Inorg. Chem.* **2007**, *46*, 8499. (d) Wang, J.-J.; Liu, C.-S.; Hu, T.-L.; Chang, Z.; Li, C.-Y.; Yan, L.-F.; Chen, P.-Q.; Bu, X.-H.; Li, Z.-M.; Wu, Q.; Zhao, L.-J.; Wang, Z.; Zhang, X.-Z. *CrystEngComm* **2008**, *10*, 681. (e) Liu, C.-S.; Chang, Z.; Wang, J.-J.; Yan, L.-F.; Bu, X.-H.; Batten, S. R. *Inorg. Chem. Commun.* **2008**, *11*, 889. (f) Liu, C.-S.; Sañudo, E. C.; Wang, J.-J.; Chang, Z.; Yan, L.-F.; Bu, X.-H. *Aust. J. Chem.* **2008**, *61*, 382. (g) Liu, C.-S.; Wang, J.-J.; Chang, Z.; Batten, S. R.; Yan, L.-F.; Bu, X.-H. *Trends Inorg. Chem.* **2008**, *10*, 81. (h) Liu, C.-S.; Wang, J.-J.; Chang, Z.; Yan, L.-F.; Hu, T.-L. *Z. Anorg. Allg. Chem.* **2009**, *635*, 523. (i) Liu, C.-S.; Wang, J.-J.; Chang, Z.; Yan, L.-F.; Bu, X.-H. *CrystEngComm* **2010**, *12*, 1833.
- (26) Chang, Z.; Zhang, A.-S.; Hu, T.-L.; Bu, X.-H. *Cryst. Growth Des.* **2009**, *9*, 4840.
- (27) Liu, C.-S.; Hu, M.; Ma, S.-T.; Zhang, Q.; Zhou, L.-M.; Gao, L.-J.; Fang, S.-M. *Aust. J. Chem.* **2010**, *63*, 463.
- (28) (a) Baxter, P. N. W.; Khoury, R. G.; Lehn, J.-M.; Baum, G.; Fenske, D. *Chem.—Eur. J.* **2000**, *6*, 4140. (b) Long, D.-L.; Blake, A. J.; Champness, N. R.; Wilson, C.; Schröder, M. *Chem.—Eur. J.* **2002**, *8*, 2026. (c) Su, C.-Y.; Cai, Y.-P.; Chen, C.-L.; Smith, M. D.; Kaim, W.; Loye, H.-C. *J. Am. Chem. Soc.* **2003**, *125*, 8595. (d) Baum, G.; Constable, E. C.; Fenske, D.; Housecroft, C. E.; Kulke, T. *Chem. Commun.* **1999**, *195*. (e) Caulder, D. L.; Powers, R. E.; Parac, T. N.; Raymond, K. N. *Angew. Chem., Int. Ed.* **1998**, *37*, 1840. (f) Baxter, P. N. W.; Lehn, J.-M.; Baum, G.; Fenske, D. *Chem.—Eur. J.* **2000**, *6*, 4510. (g) Pan, L.; Huang, X. Y.; Li, J.; Wu, Y. G.; Zheng, N. W. *Angew. Chem., Int. Ed.* **2000**, *39*, 527.
- (29) (a) Brandys, M. C.; Puddephatt, R. J. *Chem. Commun.* **2001**, *1508*. (b) Pschirer, N. G.; Curtin, D. M.; Smith, M. D.; Bunz, U. H. F.; Zur Loye, H.-C. *Angew. Chem., Int. Ed.* **2002**, *41*, 583. (c) Shin, D. M.; Lee, I. S.; Chung, Y. K. *Inorg. Chem.* **2003**, *42*, 8838. (d) Du, M.; Guo, Y.-M.; Chen, S.-T.; Bu, X.-H.; Batten, S. R.; Ribas, J.; Kitagawa, S. *Inorg. Chem.* **2004**, *43*, 1287. (e) Wenger, O. S.; Henling, L. M.; Day, M. W.; Winkler, J. R.; Gray, H. B. *Inorg. Chem.* **2004**, *43*, 2043. (f) Almeida, F. A.; Klinowski, P. J. *Inorg. Chem.* **2004**, *43*, 3948. (g) Jin, J.-C.; Wang, Y.-Y.; Zhang, W.-H.; Lermontov, A. S.; Lermontova, E. K.; Shi, Q.-Z. *Dalton Trans.* **2009**, *10181*. (h) Felloni, M.; Blake, A. J.; Hubberstey, P.; Wilson, C.; Schröder, M. *Cryst. Growth Des.* **2009**, *9*, 4685.
- (30) Martinez-Vargas, S.; Hernandez-Ortega, S.; Toscano, R. A.; Salazar-Mendoza, D.; Valdes-Martinez, J. *CrystEngComm* **2008**, *10*, 86.
- (31) Brown, E. V.; Granneman, G. R. *J. Am. Chem. Soc.* **1975**, *97*, 621.
- (32) SAINT Software Reference Manual; Bruker AXS: Madison, WI, 1998.
- (33) Sheldrick, G. M. SADABS, Siemens Area Detector Absorption Corrected Software; University of Göttingen: Göttingen, Germany, 1996.
- (34) Sheldrick, G. M. SHELXTL NT Version 5.1. Program for Solution and Refinement of Crystal Structures; University of Göttingen: Göttingen, Germany, 1997.
- (35) Wilkinson, G.; Gillard, R. D.; McCleverty, J. A., Eds.; Comprehensive Coordination Chemistry; Pergamon: Oxford, 1987; Vol. 5.

- (36) Nakamoto, K. *Infrared and Raman Spectra of Inorganic and Donor Hydrogen Bond Coordination Compounds*; John Wiley & Sons: New York, 1986.
- (37) (a) Deacon, G. B.; Phillips, R. J. *Coord. Chem. Rev.* **1980**, *33*, 227. (b) Du, M.; Zhang, Z.-H.; Zhao, X.-J.; Xu, Q. *Inorg. Chem.* **2006**, *45*, 5785. (c) Tao, J.; Tong, M.-L.; Chen, X.-M. *J. Chem. Soc., Dalton Trans.* **2000**, 3669.
- (38) Addison, A. W.; Rao, T. N.; Reedijk, J.; Rijn, J. V.; Verschoor, G. C. *J. Chem. Soc., Dalton Trans.* **1984**, 1349.
- (39) (a) Desiraju, G. R.; Steiner, T. *The Weak Hydrogen Bond in Structural Chemistry and Biology*; Oxford University Press: Oxford, 1999. (b) Calhorda, M. *J. Chem. Commun.* **2000**, 801. (c) Hobza, P.; Havlas, Z. *Chem. Rev.* **2000**, *100*, 4253.
- (40) (a) Janiak, C. *J. Chem. Soc., Dalton Trans.* **2000**, 3885 and references cited therein. (b) Hunter, C. A.; Sanders, J. K. M. *J. Am. Chem. Soc.* **1990**, *112*, 5525.
- (41) For C–H···π interactions please see (a) Nishio, M.; Umezawa, Y.; Honda, K.; Tsuboyama, S.; Suezawa, H. *CrystEngComm* **2009**, *11*, 1757. (b) Nishio, M.; Hirota, M.; Umezawa, Y. *A Comprehensive Monograph: The CH/π Interaction Evidence, Nature, and Consequences*; Wiley-VCH: New York, 1998. (c) For more details, please also refer to a website established by Nishio, M.: <http://www.tim.hi-ho.ne.jp/dionisio/>.
- (42) (a) Spek, A. L. *PLATON, A Multipurpose Crystallographic Tool*; Utrecht University: Utrecht, The Netherlands, 2005, available via <http://www.cryst.chem.uu.nl/platon> (for Unix) and <http://www.chem.gla.ac.uk/~louis/software/platon/> (for MS Windows). (b) Küppers, H.; Liebau, F.; Spek, A. L. *J. Appl. Crystallogr.* **2006**, *39*, 338.
- (43) For example: (a) Lee, H. Y.; Park, J.; Lah, M. S.; Hong, J.-I. *Cryst. Growth Des.* **2008**, *8*, 587. (b) Cheon, Y. E.; Suh, M. P. *Chem.—Eur. J.* **2008**, *14*, 3961. (c) Turner, D. R.; Strachan-Hatton, J.; Batten, S. R. *CrystEngComm* **2008**, *10*, 34. (d) Wang, C.-C.; Lin, W.-Z.; Huang, W.-T.; Ko, M.-J.; Lee, G.-H.; Ho, M.-L.; Lin, C.-W.; Shih, C.-W.; Chou, P.-T. *Chem. Commun.* **2008**, 1299. (e) Chen, B.; Fronczek, F. R.; Maverick, A. W. *Chem. Commun.* **2003**, 2166. (f) Bu, X.-H.; Tong, M.-L.; Chang, H.-C.; Kitagawa, S.; Batten, S. R. *Angew. Chem., Int. Ed.* **2004**, *43*, 192. (g) Du, M.; Zhao, X.-J.; Guo, J.-H.; Batten, S. R. *Chem. Commun.* **2005**, 4836. (h) Wang, S.; Zhang, L.; Li, G.; Huo, Q.; Liu, Y. *CrystEngComm* **2008**, *10*, 1662. (i) Wang, X.-L.; Qin, C.; Wang, E.-B.; Li, Y.-G.; Su, Z.-M. *Chem. Commun.* **2005**, 5450. (j) Xue, D.-X.; Lin, J.-B.; Zhang, J.-P.; Chen, X.-M. *CrystEngComm* **2009**, *11*, 183. (k) Brown, K. A.; Martin, D. P.; Supkowski, R. M.; LaDuca, R. L. *CrystEngComm* **2008**, *10*, 846. (l) Zhang, R.-B.; Li, Z.-J.; Cheng, J.-K.; Qin, Y.-Y.; Zhang, J.; Yao, Y.-G. *Cryst. Growth Des.* **2008**, *8*, 2562. (m) Hu, S.; Chen, J.-C.; Tong, M.-L.; Wang, B.; Yan, Y.-X.; Batten, S. R. *Angew. Chem., Int. Ed.* **2005**, *44*, 5471. (n) Huang, Y.-X.; Prots, Y.; Kniep, R. *Chem.—Eur. J.* **2008**, *14*, 1757. (o) Carlucci, L.; Ciani, G.; Macchi, P.; Prosperio, D. M. *Chem. Commun.* **1998**, 1837.
- (44) Flack, H. D. *Acta Crystallogr.* **1983**, *A39*, 876.
- (45) Piguet, C.; Bernardinelli, G.; Hopfgartner, G. *Chem. Rev.* **1997**, *97*, 2005.
- (46) (a) Pérez-García, L.; Amabilino, D. B. *Inorg. Chem.* **2007**, *36*, 941. (b) Chen, X.-Y.; Shi, W.; Xia, J.; Cheng, P.; Zhao, B.; Song, H.-B.; Wang, H.-G.; Yan, S.-P.; Liao, D.-Z.; Jiang, Z.-H. *Inorg. Chem.* **2005**, *44*, 4263. (c) Siemeling, U.; Scheppelmann, I.; Neumann, B.; Stammmer, A.; Stammmer, H. G.; Frelek, J. *Chem. Commun.* **2003**, 2236. (d) Zhang, J.-P.; Lin, Y.-Y.; Huang, X.-C.; Chen, X.-M. *Chem. Commun.* **2005**, 1258. (e) Balamurugan, V.; Mukherjee, R. *CrystEngComm* **2005**, *7*, 337. (f) Chen, X.-D.; Du, M.; Mak, T. C. W. *Chem. Commun.* **2005**, 4417.
- (47) (a) Yersin, H.; Vogler, A. *Photochemistry and Photophysics of Coordination Compounds*; Springer: Berlin, 1987. (b) Valeur, B. *Molecular Fluorescence: Principles and Applications*; Wiley-VCH: Verlag GmbH, 2001.
- (48) (a) Qiu, Y.; Li, Y.; Peng, G.; Cai, J.; Jin, L.; Ma, L.; Deng, H.; Zeller, M.; Batten, S. R. *Cryst. Growth Des.* **2010**, *10*, 1332. (b) Liang, L.-L.; Ren, S.-B.; Zhang, J.; Li, Y.-Z.; Du, H.-B.; You, X.-Z. *Cryst. Growth Des.* **2010**, *10*, 1307. (c) Zhang, L.-P.; Ma, J.-F.; Yang, J.; Pang, Y.-Y.; Ma, J.-C. *Inorg. Chem.* **2010**, *49*, 1535. (d) Liu, W.; Ye, L.; Liu, X.; Yuan, L.; Jiang, J.; Yan, C. *CrystEngComm* **2008**, *10*, 1395. (e) Zheng, S.-L.; Yang, J.-H.; Yu, X.-L.; Chen, X.-M.; Wong, W.-T. *Inorg. Chem.* **2004**, *43*, 830.